REMARKS

Claims 1 to 106 are pending in this application. Claims 1 to 22, 29, 43, 59 to 67, 69 to 84, and 103 to 106 have been withdrawn from consideration as being drawn to a non-elected invention. Claim 45 has been cancelled and claims 23, 28, 44, 46, 49 and 68 have been amended. The amended claims do not include new matter as explained below.

Claim 23 has been amended to clarify that the polynucleotide that is operably connected to a nucleic acid sequence that encodes an RNA element that modulates the stability of a transcript encoded by the polynucleotide, is not operably connected to a promoter. Support for this amendment can be found in the Specification and claims as filed, for example in paragraph [0196] to [0204] and in Example 7.

Claim 28, 44, 46, and 49 have been amended to delete reference to biologically active fragments, variants and derivatives.

Claim 68 has been amended to delete reference to the term "about".

The changes made to the Specification and Claims by the current amendment, including ~~deletions~~ and <u>additions</u>, are shown herein with deletions designated with a strikethrough and additions underlined. From the foregoing, Applicant respectfully asserts that the amendments made herein are fully supported by the specification and do not include new matter.

<u>Objections</u>

The Examiner objects to the specification because the figure legend for Figure 22 does not contain a reference to Figure 22A. The Figure has now been amended to contain such a reference, so as to obviate this objection.

With respect to objections to the claims, the Examiner objects to Claims 44 and 45 as directed to other sequences besides the elected Sequence SEQ ID NO:19. Claim 44 has been amended to be limited to SEQ ID NO:19 solely as to obviate this objections, and Claim 45 has been canceled. Accordingly, withdrawal of the objection is respectfully requested.

<u>Rejection Under 35 U.S.C.§112, first paragraph (Written Description)</u>

The Examiner has rejected Claims 28, 46, 47, and 49 as not complying with the written description requirement, allegedly because the terms, "biologically active fragments, variants or derivatives" as applied to PEST sequences and reporter proteins, are not supported by the written description. These terms no longer appear in the amended claims. Accordingly, the Examiner is

respectfully requested to withdraw the rejection of claims pursuant to 35 U.S.C.§112, first paragraph.

Rejection Under 35 U.S.C.§112, second paragraph

Claims 28, 41, 44-47 and 49 were rejected because the Examiner believed that the metes and bounds of the term "derivative" are unclear. The claims have been amended to delete this term, thereby obviating the rejection.

Claim 41 was believed indefinite because the metes and bounds of "clonable directly" are unclear. This claim has been amended to recite that the PCR products "can be directly inserted". It was well known before the filing date of the subject application that PCR products generated using non-proofreading thermostable DNA polymerases, such as native and recombinant *Taq* polymerase, lease single 3'-dA nucleotide overhangs on the reaction products. It was also well known that such products could be directly ligated into linearized vectors having ends with single 3'-dU nucleotide overhangs, which complemented the single 3'-dA nucleotide overhangs of the PCR products. Such direct insertion of PCR products, therefore, was well established and had a clear meaning to a person of skill in the art before the filing date of the present application and is explicitly taught in the present specification at least in Example 13, particularly paragraph [0296]. From the foregoing, Applicant respectfully urges the Examiner to withdraw the rejection of Claim 41 under 35 U.S.C.§112, second paragraph.

Rejection Under 35 U.S.C.§102(b)

Claims 23-26, 30, 33, 34, 36, 37, 39-42, 50-56, 68, 85, and 86 were rejected as anticipated by Shyu *et al.*, Genes and Development, 1989, Vol 3. pages 60-72. The Examiner alleges that Shyu *et al* teaches the generation of an expression vector comprising *c-fos* instability elements, (i.e., AU-rich elements or ARE), which comprise SEQ ID NO:1 and SEQ ID NO:19 and a second novel element within the *c-fos* protein coding region. The Examiner further asserts that the vector comprises the instability elements as a *c-fos*/β-globin fusion and a site into which promoters such as the β-globin or *c-fos* promoters, which are cis-acting regulatory elements that enhance transcription, have been inserted. Further, it is alleged that the half-life of the fusion protein is 28 ± 2 minutes. Applicant submits that this rejection has been rendered moot by the amendment to the claims.

Shyu *et al.*describe a system for measuring the effect of cis-acting elements (*c-fos* RNA destabilizing elements) on mRNA stability. Specifically, they disclose a construct comprising the *c-fos* promoter operably connected to a β-globin gene for cloning *c-fos* ARE (i.e., RNA stabilizing elements) into the 3' UTR of the gene. Shyu *et al.* also disclose β-globin mRNA levels over time, after activation of the *c-fos* promoter with serum. The purpose of these studies was to investigate the impact of the *c-fos* ARE on the stability of the mRNA transcribed from the β-globin gene; they were not concerned with assaying the activity of promoters. Additionally, Shyu *et al.* do not disclose the production of a vector in which the β-globin gene is operably connected to a *c-fos* ARE but is not operably connected to a promoter, wherein the vector comprises a site for insertion of promoters and other gene-expression modulating elements in operable connection with the β-globin gene. Accordingly, Shyu *et al.* fail to teach each and every element of the claim as amended.

Further, in distinct contrast to the Examiner's position, Shyu *et al.* do not disclose any polypeptides with half-lives of less than 3 hours. The half-life of 28 ± 2 minutes to which the Examiner refers is the half-life of a chimeric BBF transcript (i.e., mRNA) and not the half-life of a β-globin polypeptide. In fact, the β-globin polypeptide has a half-life of 60 days in red blood cells, where it, along with the α-globin and heme, forms hemoglobin. Applicant respectfully draws the Examiner's attention to an article by David Mendosa at the Diabetes website (Appendix A), which discloses that Hemoglobin has a half-life of 2-3 months.

In addition, when expressed in certain non-blood cells, the half-life of rabbit β–globin is reduced to 7 hrs (see, for example, Chen HY, Brinster RL. "Stability of rabbit globin and its messenger RNA in the mouse ovum." *Exp Cell Res* 1982: vol 141; pp469-72).

Consequently, Shyu *et al.* fail to disclose each and every one of the elements defined in the amended claims. For these reasons, Applicants respectfully urges the Examiner to reconsider and withdraw the rejection of claims pursuant to 35 U.S.C.§102(b).

Rejections Under 35 U.S.C.§102(e)

Newman et al.

Claims 23-26, 30, 31, 33-37, 39-41, 46, 50-55, 58 and 68 were rejected as anticipated by Newman *et al.* (Plant Cell, Vol 5, pages 701-714). The Examiner mistakenly identified Newman as prior art under §102(e), but it actually qualifies as prior art under §102(b). In any case, the

Examiner alleges that Newman *et al.* teach construction of a vector comprising a plant DST sequence (a RNA destabilizing element) that targets reporter transcripts for rapid decay. Additionally, the Examiner asserts that Newman *et al.* disclose reporter genes, including β-flucuronidase, β-globin and chloramphenicol acetyl transferase (CAT) and that the disclosed vector comprises sites for insertion of promoters as well as containing polyadenylation sequences and selectable markers. Applicant submits that this rejection has been rendered moot by the amendment to the claims.

Newman *et al.* teach constructs in which certain reporter genes are driven by the 35S promoter. They further teach the study of plant DST sequences by inserting the sequences into the 3' UTR of the CAT or β-globin genes after the 345S promoter was operably connected to these genes. Accordingly, at no stage do Newman *et al.* teach a vector in which a reporter gene is operably connected to a RNA destabilizing element but is not operably connected to a promoter, wherein the vector comprises a site for insertion of promoters and other gene-expression modulating elements in operable connection with the reporter gene. Moreover, the half-lives of β-glucuronidase and CAT polypeptides in mammalian cells are ≥ 24 hrs (see, for example Shepard *et al.*, 1983, "Receptor-mediated entry of beta glucuronidase into the parasitophorous vacuoles of macrophages infected with *Leishmania mexicana amazonensis*" *J. Exp. Med*, Vol 157, 1471-1482; Miyamoto *et al.*, 2000, "Quantitative analysis of transiently expressed mRNA in particle-bombarded tobacco seedlings" *Plant Mol. Biol. Reporter*, Vol 18, 101-107) and about 50 hours (see, e.g., Promega Notes Number 70, 1999, p.25). Copies of these articles are enclosed for the Examiner's reference in Appendix B.

Thus, Applicant's submissions in respect of Shyu *et al.* also apply to Newman *et al.* and consequently, the Examiner is respectfully urged to reconsider and withdraw the rejection of claims based on Newman *et al.* under 35 U.S.C.§102(e).

Giordano et al.

The Examiner rejects Claims 23 to 25, 30 to 37, 39 to 41, 46 to 48, 50 to 57, and 68 under 35 U.S.C. § 102(e) as being allegedly anticipated by Giordano et al. (US 2005/0091866). In particular, the Examiner asserts that Giordano et al. teach methods for identifying novel nucleic acid regulatory elements and compounds that effect regulation using vectors that comprise reporter genes such as *Renilla* luciferase, CAT and green fluorescence protein. The Examiner further asserts that UTR sequences were inserted into cloning sites to assess, for example,

sequences that affect the stability of the transcript such as destabilizing the transcript. Applicant agrees with the Examiner that Giordano et al. teach vectors for studying RNA destabilizing elements but respectfully disagrees that they disclose vectors for assaying the activity of gene expression-modulating elements such as promoters and transcriptional enhancers. This is because Giordano *et al.*, like Shyu *et al.* and Newman *et al.*, are only concerned with studying the effects of specific RNA destabilizing elements on transcript (i.e., mRNA) stability rather than with assaying the activity of different promoters. Accordingly, Applicant respectfully submits that, like the above-noted references, Giordano et al. do not teach a vector which comprises a reporter gene that is operably connected to a RNA destabilizing element and that is not operably connected to a promoter, wherein the vector comprises a site for insertion of promoters and other gene-expression modulating elements in operable connection with the reporter gene.

Additionally, Giordano et al. do not disclose any reporter proteins with half-lives of less than 3 hours. In this regard, the half-lives of *Renilla* luciferase, CAT and green fluorescence protein in mammalian cells are about 5.3 hours (see, *e.g., Promega Notes* Number *70,* 1999, p. 25), about 50 hours *(ibid)* and about 26 hours (see, *e.g.,* Corish and Tyler-Smith, 1999, Attenuation *of* green fluorescent protein half-life in mammalian cells Protein Engineering Vol 12 (12), 1035-1040), respectively. A copy of Corish and Tyler-Smith is also enclosed for the Examiner's reference see Appendix C. As such, Giordano et al. fail to disclose each and every one of the essential elements defined in the amended claims and the Examiner is respectfully urged, therefore, to reconsider and withdraw the rejection of the claims based on Giordano et al. under 35 U.S.C. §102(e).

In summary, therefore, Shyu et al., Newman et al. and Giordano et al. teach the inclusion of a putative RNA destabilizing element in a vector for the purpose of determining whether that element destabilizes RNA. However, they do not teach the use of a RNA destabilizing element for the study or measurement of transcription. Indeed their methods require prior knowledge or experimental control of transcription in order to make conclusions about mRNA stability. Further, they teach no potential uses of RNA destabilizing elements whatsoever.

Rejection of Claims Under 35 U.S.C. § 103(a)

Lorens et al. in view of Shyu et al. or Giordano et al.

The Examiner rejects claims 23 to 28, 30 to 37, 39 to 42, 44 to 48, 50 to 57, 68, and 85 to 102 as being allegedly unpatentable over Lorens et al. (US 2004/0002056) in view of Shyu *et al.*

or Giordano *et al.* Specifically, the Examiner alleges that Lorens *et al.* teach the use of self-inactivating vectors comprising reporter genes, PEST sequences and destruction boxes, but concedes that Lorens *et al.* do not teach inclusion of a RNA destabilizing element in the vectors. Nevertheless, the Examiner asserts that it would have been obvious to include the RNA destabilizing element taught by Shyu *et al.* in the vector taught by Lorens *et al.* Applicant respectfully disagrees.

As discussed above, Shyu *et al.* and Giordano *et al.* only teach the inclusion of RNA destabilizing elements for the purpose of studying the RNA destabilizing elements. Significantly, the use of RNA destabilizing elements to assay the transcriptional activity of promoters is neither taught nor suggested by Shyu *et al.* or Giordano *et al.* Further, their methods require measurement of the RNA directly, not protein and there was no teaching by either Shyu *et al.* or Giordano *et al.* as to any expected benefit of using RNA destabilizing elements for more real-time determination of transcriptional activity. Thus, in contradistinction to the Examiner's allegation, the use of RNA destabilizing elements to decrease the stability of reporter gene mRNA for permitting more real-time determination of changes in gene expression was not art-recognized but, instead, was taught for the first time by the present applicant. Accordingly, the use of RNA destabilizing elements to improve temporal correlation between protein expression and promoter activity was not within the ordinary skill in the art at the filing date of the instant application.

As such, Lorens *et al.* with either Shyu *et al.* or Giordano *et al.* do not teach all of the claimed elements because they do not teach a vector which comprises a reporter gene that is operably connected to a RNA destabilizing element and <u>that is not operably connected to a promoter</u>. Further, even if all of the claimed elements were taught by the references, it is respectfully submitted that a person of skill in the art would not have been motivated before the filing date of the present application to combine Lorens *et al.* with either Shyu *et al.* or Giordano *et al.* to arrive at the claimed constructs.

Accordingly, Applicant respectfully urges the Examiner to reconsider and withdraw the rejection of claims 23 to 28, 30 to 37, 39 to 42, 44 to 48, 50 to 57, 68, and 85 to 102 pursuant to 35 U.S.C. §103(a).

Shyu et al./Giordano et al./Lorens et al. in view of Primig et al.

The Examiner rejects claim 49 as being allegedly unpatentable under 35 U.S.C. §103(a) over Shyu *et al.* or Giordano *et al.* or Lorens *et al.* in view of Primig *et al.* (Gene, 1998, Vol. 215, pages 181-189). The Examiner asserts that coupled with the teachings of the previously cited prior art, Primig *et al.* teaches a chimeric reporter gene that encodes a fusion between GFP and neomycin phosphotransferase and that it would have been obvious to substitute the reporter and marker genes taught by Shyu *et al.* Lorens *et al.* and Giordano *et al.* with a chimeric gene of Primig *et al.* Applicant respectfully disagrees because, as discussed above, none of Shyu et al., Giordano et al. and Lorens *et al.* teach or reasonably suggest a construct in which a reporter gene is operably connected to a RNA destabilizing element but is not operably connected to a promoter, wherein the construct comprises a site for insertion of promoters and other gene-expression modulating elements in operable connection with the reporter gene.

Accordingly, Lorens *et al.* with either Shyu *et al.* or Giordano *et al.* do not teach all of the claimed elements because they do not teach a vector which comprises a reporter gene that is operably connected to a RNA destabilizing element and that is not operably connected to a promoter. Further, at the filing date of the present application, the combination of Primig *et al.* with anyone or more or Shyu *et al.* Lorens *et al.* and Giordano *et al.* would not motivate a person of skill in the art to produce the constructs defined in the amended claims. For these reasons, Applicant respectfully urges the Examiner to reconsider and withdraw the rejection of claim 49 pursuant to 35 U.S.C. §103(a).

Shyu et al./Giordano et al./Lorens et al. in view of Svensson and Akusjarvi

Claim 38 is rejected as being allegedly unpatentable under 35 U.S.C. § 103(a) over Shyu *et al.* or Giordano *et al.* or Lorens *et al.* in view of Svensson and Akusjarvi (1985, *EMBO J.* Vol. 4 (4), pages 957-964). Specifically, the Examiner asserts that Svensson and Akusjarvi teach the use of adenovirus VA RNAI on the translation of mRNAs and that it would have been obvious to one of ordinary skill in the art at the time the invention was made to add to the vector of Shyu *et al.* or Giordano *et al.* or Lorens *et al.* the VA RNAI translational enhancer taught by Svensson and Akusjarvi for analysis of gene expression in cells. Applicant respectfully traverses this ground of rejection.

As indicated above, none of Shyu *et al.* or Giordano *et al.* or Lorens *et al.* or Primig *et al.* teach or reasonably suggest a construct in which a reporter gene is operably connected to a RNA

destabilizing element and in which the reporter gene is not operably connected to a promoter, wherein the constructs comprise a site for insertion of promoters and other gene-expression modulating elements in operable connection with the reporter gene. Accordingly, a person skilled in the art, before the filing date of the present application, could not combine anyone of Shyu *et al.*, Lorens *et al.* or Giordano *et al.* with Svensson and Akusjarvi to produce a construct, as recited in the amended claims.

The Examiner is respectfully urged, therefore, to reconsider and withdraw the rejection of claim 38 pursuant to 35 U.S.C. § 103(a).

Conclusion

In view of Applicants' amendments to the claims and the foregoing Remarks, it is respectfully submitted that the present application is in condition for allowance. Should the Examiner have any remaining concerns which might prevent the prompt allowance of the application, the Examiner is respectfully invited to contact the undersigned at the telephone number appearing below.

No new matter has been added herewith. Please charge any additional fees, including any fees for additional extension of time, or credit overpayment to Deposit Account No. 11-1410.

Respectfully submitted,

KNOBBE, MARTENS, OLSON & BEAR, LLP

Dated: Feb. 18, 2005

By: _____

Jennifer A. Haynes, Ph.D.
Registration No. 48,868
Agent of Record
Customer No. 20,995
(415) 954-4114

W:\DOCS\JAH\JAH-8434.DOC
021705

Start
Directory
Food
Exercise
Medication
Meters
Basics
Complications
People
Mac Users
Newsletter

Are You "In Charge" of Your Blood Glucose?

By David Mendosa

Someone on the alt.support.diabetes newsgroup recently generated more heat than anyone else with her message. "I've never known a diabetic who used one of those things," she quotes her husband as saying about her blood glucose meter. "Diabetics get treatment from their doctors. They don't need this meter nonsense."

To her husband, using a blood glucose meter is a sign of health fanaticism, she reports. Actually, as misguided as this man is, this is a good reminder that not everyone knows the benefits of tight control and how to get it.

You have to know your blood glucose levels.

Two long-term studies completed in the past few years—one of people with type 1 diabetes and the other of those with type 2—proved that tight control dramatically reduces the possibility of complications. To get that tight control you have to know what your blood glucose levels are.

Finger sticks with a blood glucose meter help in telling us how we are doing. But they measure only one point in time. Another test measures glycated hemoglobin or HbA1c. Since hemoglobin has a half-life of two to three months, this test indicates the level of control over that extended time period.

Now there is a third, intermediate option for testing. LXN Corp. (pronounced Lex-in) in San Diego, California, recently introduced the In Charge™ meter. This new meter measures both blood glucose and something called fructosamine (LXN calls it GlucoProtein®). It is the

only meter on the market to offer both tests.

Fructosamine is similar to HbA1c in that both indicate the average of continuous blood glucose changes over a period of time. But the fructosamine test measures a shorter window of two to three weeks, allowing you to more quickly discover if your glycemic control is slipping and lets you and your doctor respond with diet, exercise, or medication as appropriate.

LXN sent me one of the first meters off the production line, and I have been testing every week since September 21. I have found the In Charge meter to be very useful. The In Charge is actually a second generation of fructosamine-testing meters.

The Duet Came First

LXN introduced the first meter that tests fructosamine about a year and a half ago. I reviewed that meter, the Duet, for the February 1999 issue of Diabetes Wellness Letter. Anyone who read that article could see how lukewarm I was about the Duet.

The Duet was a large, expensive, clunky machine that was too sensitive to the tester following the correct technique of collecting a huge drop of blood—25 microliters—through a straw. The In Charge meter is a significant improvement from the Duet, which LXN markets only to health care professionals.

The In Charge meter is in fact the first home meter to measure fructosamine. The system, including an initial supply of both glucose and fructosamine test strips, lists for $79.95, and like most meter manufacturers LXN offers a rebate and trade in. The rebate is $20 and the trade in is $45.

The blood drop for the fructosamine test is much less than that required by the Duet meter, but is still a fairly large drop at 15 microliters. But unlike the Duet meter no straw is required. Also, the blood drop needed to do a standard blood glucose test with the In Charge meter is significantly smaller than that needed for the fructosamine test (six microliters).

Lower than Expected Numbers

In my experience with the In Charge meter to test fructosamine,

numbers were lower than I expected (except for the week I had a cold), based on my finger stick results which I was still conducting with my usual meter. I always took my blood glucose tests the first thing in the morning. Those fasting numbers were looking so bad—in the 140s and 150s—that I got a HbA1c test and was sure that my endocrinologist would prescribe oral medication or insulin.

I should have believed the fructosamine results. They averaged about 220, which is the equivalent of an HbA1c of between 5 and 6, according to the conversion chart produced by LXN. The HbA1c test I got in mid-November was 5.4.

That made a believer out of me.

Accuracy does not appear to be a big consideration. Fructosamine test variability is inherently greater than glucose test variability. The key is that trend information is more valuable than is single-test information.

I still have some reservations about the In Charge meter. The biggest problem for me is that it is sometimes difficult to get a large enough blood sample.

Derek Paice, a retired engineer in Palm Harbor, Florida, notes a few other things you have to be careful with. You can't milk your finger like you do with a blood glucose test, because that will cause hemolysis—a modification of red blood cells in which hemoglobin is liberated—which raises the reading. Also, drinking alcohol or taking 1000 mg of vitamin C in the previous five hours will impact test results.

Teri Robert, who lives in Washington, West Virginia, just got her In Charge meter. Her doctor encouraged her to get it. "My initial impression is pretty good," she tells me. "It's compact and easy to use."

Two Control Tests Onerous

What she doesn't like is the recommendation for running two control tests (labeled "normal" and "high") every time you open a new vial. A way around this is to buy GlucoProtein test strips together with glucose strips in LXN's Value Pack, which includes 50 glucose test strips and four GlucoProtein test strips at a suggested list price of

$36.95. That compares quite favorably with other manufacturers' glucose-only strip pricing, which averages $35 per 50 glucose strips. That provides the GlucoProtein strips at little or no extra cost.

But if more strips came in each vial, the requirement would be less onerous. And, of course, not everyone does all the recommended control tests.

Another user, Richard Aleksander in Austin, Texas, emphasizes the other test that the In Charge meter performs, a regular blood glucose test. He likes the speed. "I can perform a test while walking around or sitting at a stoplight in traffic," he says. "Low readings are reported in five seconds or less. High BGs take durations approaching 15 seconds."

The In Charge meter can, indeed, test blood glucose faster than any other meter on the market. It requires a six microliter blood sample, while several other new blood glucose meters need only 2 or 3 microliters. But the more I used this little meter with its clear, large display the more I like it for testing both my blood glucose and fructosamine.

The meter's memory is another plus. The In Charge stores the most recent 200 glucose tests results and 50 fructosamine test results with the date and time. You will soon be able to automatically upload these test results to glucose and fructosamine tracking software on the LXN Web site, http://www.inchargenow.com/. I am currently beta testing the software and data cable used to connect the meter to a PC. This is something that no other meter offers.

Using the In Charge meter to test your fructosamine and blood glucose—or just your fructosamine, if you are happy with your current meter—won't make a fanatic out of you. It will give you the chance to see the results of any recent changes in your diet or medication and alert you if you need to contact your doctor before your next scheduled visit. And it will give you the knowledge you need to keep in charge of your diabetes and prevent or postpone all those complications that we would rather not get.

This article appeared originally on the DiabetesWebSite.com, which is no longer on-line.

Update

In 2002 LifeScan bought LXN and discontinued all of its products including the In Charge and Duet meters. It also recalled all GlucoProtein (fructosamine) test strips because they may produce false highs.

Last modified: August 21, 2002

 Go back to David Mendosa's Home Page

 Go back to David Mendosa's Diabetes Directory

I subscribe to the HONcode principles of the Health On the Net Foundation

David Mendosa
4455 Chippewa Drive
Boulder, Colorado 80303
E-mail: mendosa@mendosa.com
Telephone: (303) 494-2036

RECEPTOR-MEDIATED ENTRY OF β-GLUCURONIDASE INTO THE PARASITOPHOROUS VACUOLES OF MACROPHAGES INFECTED WITH *LEISHMANIA MEXICANA AMAZONENSIS**

BY VIRGINIA L. SHEPHERD,‡ PHILIP D. STAHL, PAULETTE BERND,§ AND MICHEL RABINOVITCH

From the Department of Physiology and Biophysics, Washington University School of Medicine, St. Louis, Missouri 63110; and the Departments of Cell Biology and Pharmacology, New York University School of Medicine, New York 10016

Leishmania are protozoa that infect humans and certain other mammals in tropical and subtropical countries. Different species and subspecies of the parasite induce a wide spectrum of cutaneous, mucocutaneous, or visceral disease. The nonflagellated form of the parasite, the amastigote, is essentially an obligatory parasite of mononuclear phagocytes (1, 2). Infected macrophages can survive for at least several weeks in culture and the infection is quite compatible with replication of the host cells (3). *Leishmania* amastigotes lodge and multiply within parasitophorous vacuoles (p.v.),[1] assumed to be modified phagolysosomes. This assumption is supported by experiments in which the secondary lysosomes of macrophages were loaded with electron-dense tracers such as thorium dioxide or saccharate iron oxide before infection of the cultures with *Leishmania*. Transmission electron microscopy revealed the presence of the colloids within the p.v. and images suggesting fusion of the labeled secondary lysosomes with the vacuoles were also documented (4–6). However, only rarely was electron-dense acid phosphatase product detected in the lumen of the p.v. (4, 5, 7).

Macrophages infected with *Leishmania* thus provide an interesting system to determine how intracellular parasites may affect the numbers, function, synthesis, assembly, and recirculation of the vacuolar and lysosomal components of the host cell. In the present study we show that radioiodinated rat preputial gland β-glucuronidase, a ligand recognized and internalized via macrophage surface receptors specific for mannose-terminated ligands (8, 9), can enter the parasitophorous vacuoles when given to macrophage cultures either before or after infection with *L. mexicana amazonensis*. We chose this species of *Leishmania* because of the large size of the vacuoles it induces in the host cells.

* Supported by a grant from the Cystic Fibrosis Foundation to V. Shepherd, a grant from the Muscular Dystrophy Association to P. Stahl, and grants AI 19341 (to Dr. Shepherd), GM 21096 and CA 12858 (to Dr. Stahl), and AI 10969 (to M. Rabinovitch).

‡ Fellow of the Parker Francis Foundation.

§ Postdoctoral Fellow of the Pharmaceutical Manufacturers Association Foundation.

[1] *Abbreviations used in this paper*: DME, Dulbecco's modified Eagle's minimum essential medium; FBS, fetal bovine serum; HS, horse serum; LCM, L cell-conditioned medium; man-BSA, mannose-bovine serum albumin; p.v., parasitophorous vacuoles; PBS, phosphate-buffered, Ca-, Mg-free saline; TCA, trichloroacetic acid.

Materials and Methods

Animals. Adult golden hamsters were bred at and provided by the Division of Parasitology, New York University School of Medicine. Female Swiss-Webster mice, 20–25 g body weight were purchased from Taconic Farms, Inc., Germantown, NY.

Media. Ca^{++}, Mg^{++}-free phosphate-buffered saline (PBS) contained 5 mm potassium phosphate buffer and 138 mM NaCl and was adjusted to pH 7.2. Dulbecco's modified Eagle's minimal essential medium (DME), horse serum (HS), and fetal bovine serum (FBS) were obtained from Gibco Laboratories, Grand Island, NY. Conditioned medium (LCM) was collected from confluent L cell fibroblast cultures incubated for 7 d in serum-free medium (10).

Preparation of the Ligands. β-glucuronidase was purified to homogeneity from rat preputial glands (11). Mannose-bovine serum albumin (Man-BSA) was prepared as described elsewhere (12) and contained 20–40 mol of sugar per ml of protein. Ligands were iodinated by the chloramine T method (13) to a specific activity of 1–10 μCi/μg.

Leishmania Strain and Preparation of the Amastigote Inoculum. *L. mexicana amazonensis* LV 79, originally obtained from the Dept. of Parasitology, Liverpool School of Tropical Medicine, England, was kindly provided by Dr. J. P. Dedet (Institut Pasteur, Paris). Amastigote suspensions were injected subcutaneously in the paws of hamsters, and 4–6 wk later the granulomas were excised and minced. Tissue debris was removed by slow centrifugation (40 *g*, 10 min), and the parasites were recovered and washed by three centrifugation cycles at 1,000 *g* for 10 min (10).

Macrophage Cultures. Bone marrow-derived macrophages were obtained by explanting 1.5 × 10^6 mouse bone marrow cells into each of 16-mm diam wells of Cluster plates (Costar, Data Packaging, Cambridge, MA) containing 0.5 ml of DME enriched with 10% HS, 10% of LCM, 50 U of penicillin, and 50 μg/ml of streptomycin. The cultures were used on the 5th d, at which time they contained between 3 × 10^5 and 5 × 10^5 macrophages. For light microscopic radioautography, cells were grown on 13-mm glass coverslips placed in the wells. For electron microscopic radioautography, cells were grown in 35-mm dishes, and for radiometric determinations of ligand uptake and degradation, macrophages were grown directly on tissue culture plastic in cluster plates. Macrophages were grown at 37°C in a humidified 5% CO_2-air atmosphere.

Infection of the Macrophage Cultures. The parasites were suspended in DME containing 10% FBS and 2.5% LCM, and the cultures were infected with an estimated multiplicity of two to three amastigotes per macrophage. Since the strain of *Leishmania* used is temperature sensitive (14), infected cultures were transferred to an incubator adjusted to a temperature of 34°C. The percent of infection varied between 50 and 80% in different experiments.

Uptake Studies. For time course studies, ^{125}I-β-glucuronidase was added to each well containing 0.4 ml DME, with 10% S, 2.5% LCM, and 10 mM Hepes. Ligand was added at a concentration of 20 μg/ml (containing cold carrier) and a specific activity of 3–4 × 10^5 cpm/μg. To determine nonspecific uptake, companion wells received 1 mg/ml mannan. For studies using ^{125}I-Man-BSA as the ligand, Man-BSA was added at a concentration of 1 μg/ml (with added cold) and ~10^6 cpm/μg. At various times after addition of the ligand, the medium was removed (for degradation studies) and the cells were washed twice with PBS. The cell monolayers were solubilized in 0.1% Triton X-100 and counted by means of a gamma counter. Ligand degradation (using Man-BSA) was measured by determining the radioactivity liberated from Man-BSA in the culture medium after precipitation with trichloroacetic acid (TCA) (15).

Radioautography. For radioautography experiments, ligand additions were as follows: β-glucuronidase was added at 20 μg/ml and a specific activity of ~2.5 × 10^5 cpm/μg (2 × 10^5 cpm/well); Man-BSA was added at 1 μg/ml and ~6 × 10^5 cpm (2 × 10^5 cpm/well). For time course studies, macrophage cultures (1–2 d postinfection) were incubated with labeled ligands for periods of time between 30 min and 50 h. Uninfected macrophages were similarly treated. In pulse-chase experiments, infected and noninfected macrophages were incubated with ligand for 18 h, washed, and incubated in ligand-free medium for varying periods of time before fixation. In "pre-load" experiments, cultures were incubated with ^{125}I-β-glucuronidase, washed, infected, and maintained in ligand-free medium until fixation.

For light microscopic radioautography, after incubation with ligand the macrophages on coverslips were washed three times with PBS and fixed for 30 min at room temperature with

either 9:1 ethanol/acetic acid or 2% glutaraldehyde in PBS. After fixation the cultures were washed in distilled water, dried, and the coverslips were attached to microscope slides by means of 'Permount' (Fisher Scientific Co., Pittsburgh, PA). The slides were coated with NTB-2 nuclear track emulsion (Eastman Kodak Co., Rochester, NY) (16). After an exposure of 2–4 d, the emulsion was developed in D19, fixed, and the cells were lightly counterstained with Diff Quick (American Scientific Products Div., American Hospital Supply Corp., McGraw Park, IL).

For electron microscopic radioautography, macrophages cultivated on 35-mm dishes after incubation with the ligand were fixed in glutaraldehyde, postfixed in 1% osmium tetroxide, stained with magnesium uranyl acetate, and embedded in Epon 812 (Ernest F. Fullam, Inc., Schenectady, NY). Representative areas were cut out and re-embedded. Pale gold sections were prepared and coated with Ilford *L4* emulsion (Polysciences, Inc., Warrington, PA) as described elsewhere (17). After a 2-wk exposure the emulsion was developed with D19 and fixed. The sections were picked up on 200 mesh grids, stained with uranyl acetate and lead citrate, and viewed with a JEOL 100 S electron microscope.

Results

Light Microscopic Radioautography. Marrow-derived macrophage cultures were established on coverslips and infected with *Leishmania*. 1 or 2 d after infection, ^{125}I-β-glucuronidase was added to the cultures. At various intervals between 30 min and 50 h, the monolayers were fixed and processed for light microscopic radioautography. To determine whether the uptake was mediated by the mannose receptor, some cultures were incubated with the ligand in the presence of 1 mg/ml mannan.

Radioautographs of infected macrophages were scored as positive when the grain density over the p.v. was detectably higher than the grain density over both the remainder of the cell and the intercellular background. This criterion could be met within a large range of grain densities overlying the vacuoles. In the usual preparations, 5–10 grains over a medium sized vacuole (80–100 μm^2) defined a lightly but definitely labeled infected cell. Positive vacuoles were rarely found before 4 h of incubation with the ligand. Consistent labeling was observed at 4 h and at later time periods. Fig. 1 summarizes the results of three separate experiments and shows that the percent of macrophages bearing at least one positive vacuole increased with the incubation time, from ~15% at 4 h to ≥80% at 50 h. At each time period grain densities varied markedly between different vacuoles, but as the incubation time increased, the proportion of heavily labeled vacuoles (>50 grains per 100 μm^2) increased. Figs. 2 a and b provide examples of positive radioautographs over the p.v.

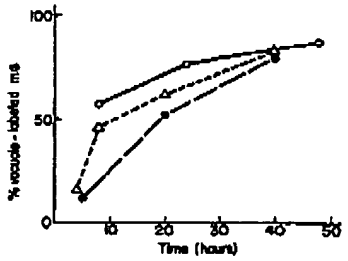

FIG. 1. Light microscopic radioautography of macrophages infected with *L. mexicana amazonensis*. Percent of macrophages with labeled parasitophorous vacuoles as a function of the length of incubation of the cultures with ^{125}I-β-glucuronidase. The curves summarize the results of three separate experiments. Each point represents the average of 2–4 coverslips, with at least 50 macrophages scored per coverslip.

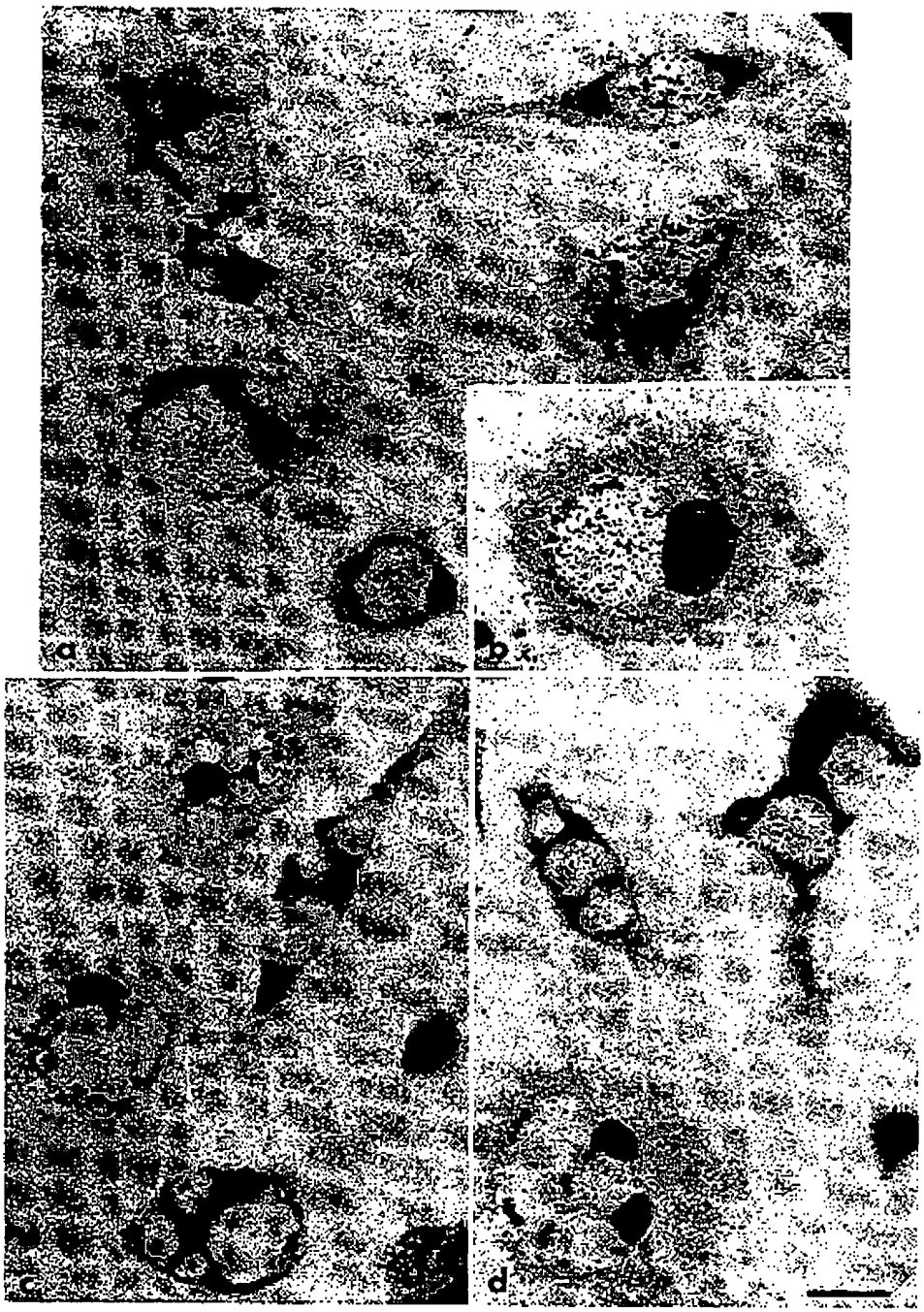

FIG. 2. Light microscopic radioautographs of macrophages incubated with radiolabeled β-glucuronidase. The length of the bar represents 10 μm. a, b, and c show macrophages fixed 20 h after continuous incubation with the ligand. (a) Microscope field with six macrophages displaying labeled p.v. Arrowhead points to *Leishmania* amastigote. Note the scarcity of grains over the non-p.v. cytoplasm. (b) Well-infected macrophage with high grain density over p.v. and a clearly but less labeled cytoplasm. (c) Macrophages incubated with the ligand for 20 h in the presence of 1 mg/ml mannan. Very few grains are seen over the cells. (d) Macrophages preloaded with the radiolabeled ligand for 5 h, washed, infected, and cultivated for 48 h without any added ligand. Moderate but definite labeling of the p.v.

of macrophages incubated with the ligand for 20 h. In most instances (Fig. 2 a) infected cells had few grains over the cytoplasm (besides the grains over the p.v.). In only a few cells (e.g., Fig. 2 b) was the non-p.v. cytoplasm moderately labeled. Furthermore, addition of mannan with the ligand (Fig. 2 c) markedly reduced both the percent of labeled macrophages (e.g., from 80% to 15%, averages of triplicates) and the grain density over the positive vacuoles.

The results indicate that an exogenous ligand accumulates and persists within the parasitophorous vacuoles, but they do not demonstrate the means of delivery of the ligand. The ligand could be transferred to p.v. by fusion of prelysosomal vesicles, of secondary lysosomes with the vacuoles, or by a combination of these mechanisms. To determine if ligand could be transferred to vacuoles from preformed lysosomes, the following preloading experiment was performed. Noninfected macrophages were incubated with ^{125}I-β-glucuronidase for 5 or 18 h, washed, infected, and cultivated for an additional period of 48 h in the absence of added ligand. In a typical experiment, after a loading period of 18 h, 54% of the infected macrophages displayed labeled parasitophorous vacuoles (average of three coverslips). Fig. 2 d illustrates positive p.v. radioautographs in macrophages preloaded with the ligand for 5 h, washed, infected, and fixed after an additonal culture period of 48 h. Since the bulk of the internalized ligand should have been delivered to the lysosomal compartment during the preloading period, this result indicates that secondary lysosomes can fuse with and deliver ligand to the p.v. The possibility that prelysosomal vesicles also carried ligand to the vacuoles cannot be excluded but is improbable in view of the prolonged incubation of cells with ligand that was required for detectable labeling of the vacuoles in time course experiments (Fig. 1).

Pulse-chase Experiments. To evaluate the persistence of the label in p.v., infected macrophages were pulsed with ligand for 24 h, washed, incubated in ligand-free medium, and fixed at varying periods thereafter. In one such experiment, the percent of macrophages with positive p.v. after postincubation for 8, 24, or 48 h was respectively 85, 83, and 39 (averages of triplicates). Grain density over the vacuoles was distinctly reduced in the 48-h group. Thus, some ligand appeared to be associated with vacuoles for at least 48 h after a 24-h period of exposure to the ligand. This result agrees with the known stability of internalized β-glucuronidase (13).

Electron Microscopic Radioautography. The light microscopic observations suggested but did not prove that ligand was taken up into the p.v. Indeed, the grains could have arisen from label distributed around but not within the vacuoles. The true vacuolar location of the ligand was confirmed by means of radioautography at the electron microscopic level. Control and infected macrophages were incubated with ^{125}I-β-glucuronidase for 20 h, washed, fixed, and embedded in Epon, and thin sections were processed for electron-microscope radioautography. Fig. 3 shows a radioautograph of a noninfected macrophage. The cell, which was fixed after 20 h of incubation with the ligand, displays numerous silver grains mostly associated with secondary lysosomes. Fig. 4 shows a low magnification picture of a radioautograph of an infected macrophage similarly incubated with the radiolabeled ligand; most of the grains are associated with the p.v. Two pictures of radioautographs of infected macrophages, taken at a higher magnification, are shown in Figs. 5 a and b. Again, silver grains are predominantly associated with the p.v. While a few grains are present over the remaining cytoplasm, they are not clearly associated with secondary lysosomes.

FIG. 3. Electron microscopic radioautograph of noninfected macrophage incubated with radiolabeled β-glucuronidase for 20 h before fixation. Silver grains are mainly associated with dense secondary lysosomes. Bar indicates 1 μm.

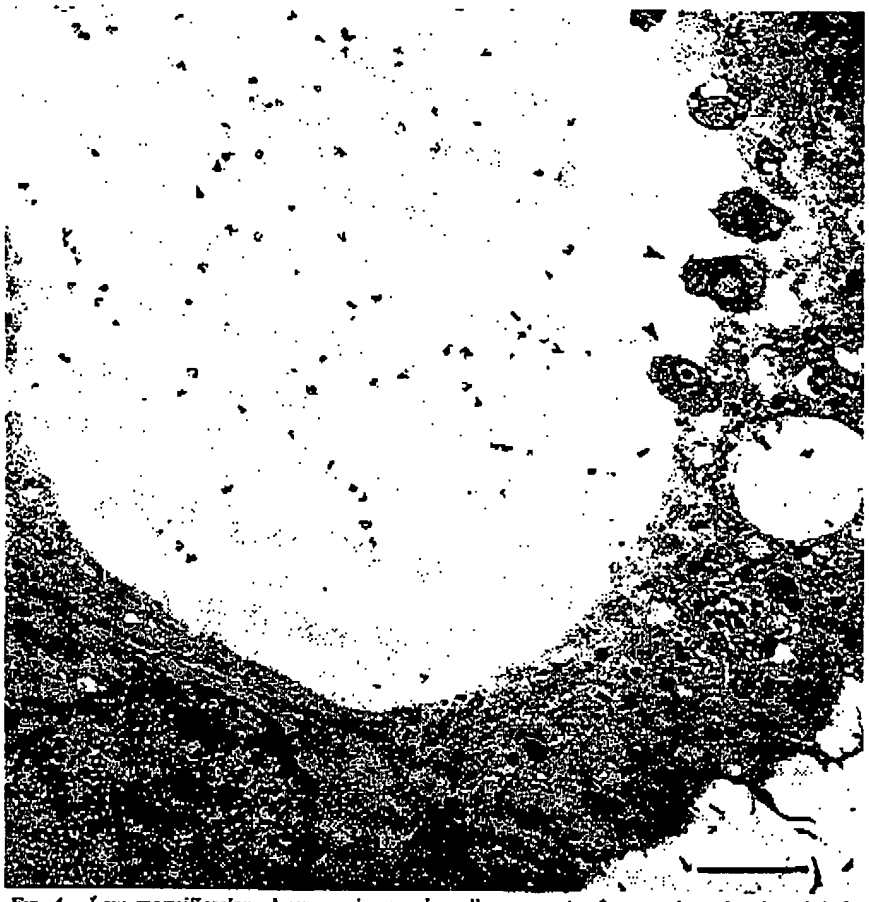

FIG. 4. Low magnification electron microscopic radioautograph of macrophage incubated 1 d after infection with radiolabeled β-glucuronidase for 20 h and fixed. The bar represents 5 μm. *Leishmania* amastigotes indicated by arrowheads. Silver grains are present mainly over the lumen of p.v.

Studies with ^{125}I-Man-BSA. Experiments similar to those described above were performed with infected macrophages incubated with ^{125}I-man-BSA, a ligand rapidly degraded after uptake via the mannose receptor (13). In no instance were p.v. distinctly labeled after incubation of macrophages with the iodinated man-BSA. Together with the uptake studies summarized below, these experiments show that man-BSA, in contrast with β-glucuronidase, is rapidly degraded within the lysosomal compartment and this probably precludes delivery of the ligand to the p.v.

Uptake Studies. Infected and noninfected macrophage cultures were incubated with iodinated β-glucuronidase or man-BSA. At different time periods cell-associated counts (for both ligands) or TCA-soluble counts (for man-BSA) were determined. Counts are expressed as percentage of the initial input after correction for mannan controls. In the experimental results summarized in Fig. 6, it can be seen that the

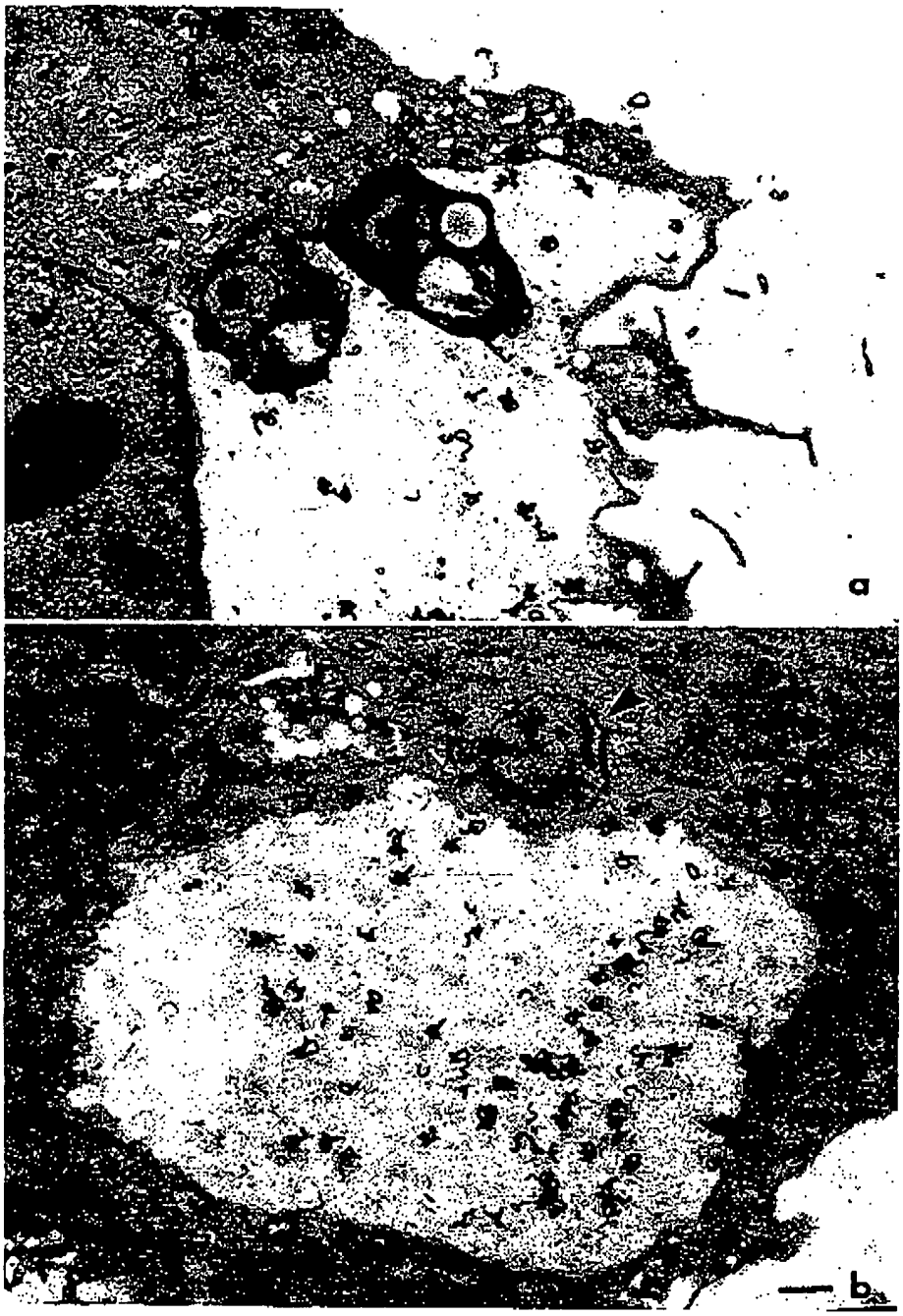

FIG. 5. Electron microscopic radioautographs of infected macrophages, from the same preparation as Fig. 4. Bar represents 1 μm. In both a and b most grains are found over p.v. The few grains over the cytoplasm are not clearly associated with secondary lysosomes. A tangentially cut Leishmania is indicated by arrow in b.

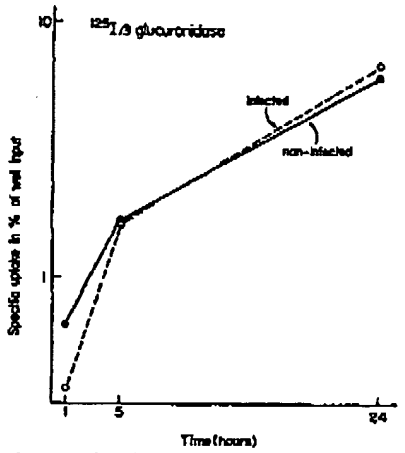

FIG. 6. Uptake of ^{125}I-β-glucuronidase by marrow-derived macrophages. 1.38×10^9 cpm were added per well containing ~5×10^6 macrophages with a 50% infection.

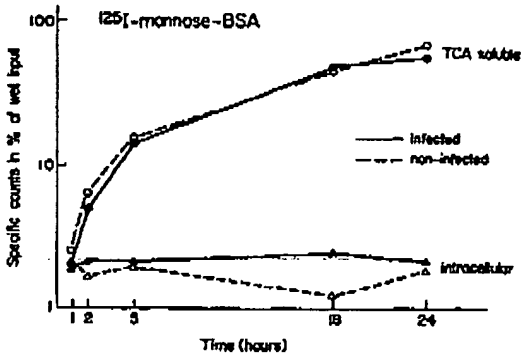

FIG. 7. Uptake and degradation of ^{125}I-mannose-BSA by marrow-derived macrophages. 2.9×10^9 cpm added per well. Same experiment as Fig. 6.

uptake of β-glucuronidase increased as the incubation period progressed. In contrast, man-BSA was rapidly degraded, with a time course of uptake showing increasing accumulation of TCA-soluble counts in the medium (Fig. 7). In each case the time course of uptake was similar in infected and noninfected cells.

Discussion

We have demonstrated that β-glucuronidase is taken up by macrophages infected with *Leishmania* and penetrates the parasitophorous vacuoles. Since this conclusion rests on the distribution of grains in light and electron microscopic radioautographs, the proportion of the radioactivity in the p.v. associated with intact as opposed to partially degraded enzyme molecules is not yet known. The semi-quantitative radioautographic observations of the persistence of the label in many vacuoles 24–48 h after removal of the ligand from the culture medium certainly supports the relatively long intracellular life of the enzyme in the present experiments.

The fate of the mannose receptor-ligand complex in macrophages has been studied in detail (13, 18). Once bound to the cell surface receptor, ligand is internalized (at 37°C) and delivered to lysosomes, while the receptor recycles back to the cell surface. Apparently, receptor-ligand complexes move into an acidic, presumably prelysosomal vesicle, where dissociation of the complex occurs, although the actual mechanism involved in these steps is unknown. After receptor-ligand dissociation, the ligand could be transferred to *Leishmania*-containing vacuoles by fusion with prelysosomal vesicles or of secondary lysosomes. The fact that vacuolar labeling was also observed in experiments where the cells were first loaded with β-glucuronidase and then infected suggests that the ligand had been delivered to secondary lysosomes and was then transferred through fusion to the p.v. This result agrees with previous observations using electron-opaque tracers (4–6). Although the present data support transfer from secondary lysosomes, delivery by means of prelysosomal ligand-containing vesicles cannot be excluded.

An interesting observation relates to the scarcity of grains over the cytoplasm of infected cells that carried labeled p.v. (Figs. 2, 4, and 5). In these and in previous ultrastructural studies (7), fewer lysosomes were also seen in the cytoplasm of infected cells. In addition, a clear reduction in the number of acid phosphatase or aryl-sulfatase positive granules was seen in the cytoplasm of *Leishmania*-infected peritoneal macrophages (C. B. Mestriner and M. Rabinovitch, manuscript in preparation). Thus, the reduction in the cytoplasmic label in infected macrophages may be related to the diminished number of lysosomes in the infected cell. It remains to be seen whether this apparent reduction in lysosome numbers is related to lysosome fusion with the p.v. and/or with the plasma membrane. Another possibility is that the reduction follows the inhibition of the synthesis or assembly of lysosomal components in infected cells.

Finally, in vivo studies have shown that β-glucuronidase is rapidly cleared from the circulation by Kupffer cells of the liver (19). Since this ligand accumulates within the p.v., it may be possible to devise mannosylated compounds able to target leishmanicidal drugs to the p.v. of infected macrophages.

Summary

^{125}I-labeled rat preputial gland β-glucuronidase was shown by light and electron microscopic radioautography to accumulate within the parasitophorous vacuoles of in vitro derived bone marrow macrophages infected with *Leishmania mexicana amazonensis*. β-glucuronidase uptake was mediated by the mannose receptor, since the penetration of the ligand was inhibited by mannan. Uptake was detected as soon as 4 h after incubation of infected cells with the ligand, and increased at 24 and 48 h. The label persisted in the vacuoles for at least 24 h after a 24-h pulse with the ligand, a finding compatible with the relatively long half-life of labeled β-glucuronidase in normal macrophages. Parasitophorous vacuoles were also labeled in macrophages exposed to the ligand only before infection, indicating that secondary lysosomes containing the ligand fused with the parasitophorous vacuoles. Another mannosylated ligand, mannose-BSA, which, in contrast to β-glucuronidase, is rapidly degraded in macrophage lysosomes, did not detectably accumulate in the vacuoles. The results support and extend information previously obtained with electron opaque tracers that emphasizes the phagolysosomal nature of *Leishmania* parasitophorous vacuoles. In

addition, the results suggest that appropriate mannosylated molecules may be used as carriers for targeting of leishmanicidal drugs to the parasitophorous vacuoles of infected macrophages.

We wish to thank Ms. Mary Jo DeStefano, Ms. Gail Topper, and Ms. Diane Biegel for assistance during the course of these experiments and Ms. Joyce Mixon for help with the manuscript.

Received for publication 5 January 1983.

References

1. Hommel, M. 1978. The genus *Leishmania*: biology of the parasites and clinical aspects. *Bull. Inst. Pasteur.* 75:5.
2. Mauel, J. 1980. The biology of the macrophage-*Leishmania* interaction. *In* The Host-Invader Interplay. H. van den Bossche, editor. Elsevier/North-Holland Biomedical Press, Amsterdam. 165–177.
3. Berens, R. L., and J. J. Marr. 1979. Growth of *Leishmania donovani* amastigotes in a continuous macrophage-like cell culture. *J. Protozool.* 26:453.
4. Alexander, J., and K. Vickerman. 1975. Fusion of host cell secondary lysosomes with the parasitophorous vacuoles of *Leishmania mexicana* infected macrophages. *J. Protozool.* 22:502.
5. Lewis, D. H., and W. Peters. 1977. The resistance of intracellular *Leishmania* parasites to digestion by lysosomal enzymes. *Ann. Trop. Med. Parasitol.* 71:295.
6. Berman, J. D., T. B. Fioretti, and D. M. Dwyer. 1981. In vivo and in vitro localization of *Leishmania* within macrophage phagolysosomes: use of colloidal gold as a lysosomal label. *J. Protozool.* 28:239.
7. Ryter, A., J. P. Dedet, and M. Rabinovitch. 1983. *Leishmania mexicana amazonensis*: acid phosphatase ultrastructural cytochemistry of infected mouse macrophage cultures treated with phenazine methosulfate. *Exp. Parasitol.* In press.
8. Stahl, P. D., J. S. Rodman, M. J. Miller, and P. H. Schlesinger. 1978. Evidence for receptor-mediated binding of glycoproteins, glycoconjugates, and lysosomal glycosidases by alveolar macrophages. *Proc. Natl. Acad. Sci. USA.* 75:1399.
9. Shepherd, V. L., E. J. Campbell, R. M. Senior, and P. D. Stahl. 1982. Characterization of the mannose/fucose receptor on human mononuclear phagocytes. *J. Reticuloendoth. Soc.* 32:423.
10. Rabinovitch, M., J. P. Dedet, A. Ryter, R. Robineaux, C. Topper, and E. Brunet. 1982. Destruction of *Leishmania mexicana amazonensis* amastigotes within macrophages in culture by phenazine methosulfate and other electron carriers. *J. Exp. Med.* 155:415.
11. Himeno, M., H. Ohara, Y. Arakawa, and K. Kato. 1978. β-Glucuronidase of rat preputial gland. *J. Biochem. (Tokyo).* 77:427.
12. Lee, Y. C., C. Stowell, and M. J. Krantz. 1976. 2-Imino-2-methoxyethyl 1-thioglycosides: new reagents for attaching sugars to proteins. *Biochemistry.* 15:3956.
13. Stahl, P. D., P. Schlesinger, E. Sigardson, J. Rodman, and Y. C. Lee. 1980. Receptor-mediated pinocytosis of mannose glycoconjugates by macrophages: characterization and evidence for receptor recycling. *Cell.* 19:207.
14. Biegel, D., and M. Rabinovitch. 1982. Temperature sensitivity of the incorporation of 3H uracil into nucleic acids of *Leishmania mexicana amazonensis*. *J. Cell Biol.* 95:473*a*. (Abstr.)
15. Stahl, P., and S. Gordon. 1982. Expression of a mannosyl-fucosyl receptor for endocytosis on cultured primary macrophages and their hybrids. *J. Cell Biol.* 93:49.
16. Rogers, A. W. 1979. Techniques of Autoradiography. Elsevier/North-Holland Biomedical Press, Amsterdam. 351.
17. Bernd, P., and L. A. Greene. 1983. Electron microscopic radioautographic localization of

iodinated nerve-growth factor bound to and internalized by PC12 cells. *J. Neurosci.* In press.
18. Tietze, C., P. Schlesinger, and P. Stahl. 1982. Mannose-specific endocytosis receptor of alveolar macrophages: demonstration of two functionally distinct intracellular pools of receptor and their roles in receptor recycling. *J. Cell. Biol.* 92:417.
19. Schlesinger, P. H., T. W. Doeber, B. F. Mandell, R. White, C. DeSchryver, J. S. Rodman, M. J. Miller, and P. Stahl. 1978. Liver Kupffer cell mediated plasma clearance of glycoproteins and lysosomal glycosidases, β-glucuronidase and *N*-acetyl-b-D-glucosaminidase. *Biochem. J.* 176:103.

Plant Molecular Biology Reporter 18: 101–107, 2000

Protocols

Quantitative Analysis of Transiently Expressed mRNA in Particle-Bombarded Tobacco Seedlings

TETSUYA MIYAMOTO[1], TAKAHIRO NAKAMURA[2], ISSEI NAGAO[2] and JUNICHI OBOKATA[1,*]

[1]Center for Gene research, Nagoya University, Nagoya, 464-8602 Japan; [2]Division of Bioscience, Graduate School of Environmental Earth Science, Hokkaido University, Sapporo 060-0810 Japan

Abstract. This study demonstrates that quantitative RT-PCR can be used to measure transient expression of genes introduced into plant cells by particle bombardment. An expression construct for β-glucuronidase was introduced into tobacco seedlings by particle bombardment followed by real-time quantitative RT-PCR of β-glucuronidase mRNA using a fluorogenic TaqMan probe. β-glucuronidase mRNA expression peaked within 2 h after gene transfer. β-glucuronidase protein activity was maximally elevated in plant cells 8 h after gene transfer and remained elevated for up to 50 h. This method is very sensitive, quantitating the target GUS transcript in 10 pg total RNA.

Key words: fluorogenic probe, particle bombardment, quantitative RT-PCR, transient expression

Abbreviations: GUS, β-glucuronidase.

Introduction

In studying the expression of foreign genes in plants, transient expression assay is a timesaving alternative to making stable transgenic plants. Particle bombardment is a useful method for gene delivery in this assay. This method can be applied to a wide variety of plant materials and requires no special pretreatment of the plants. One disadvantage of particle bombardment is that DNA is only introduced and expressed in cells near the plant surface. Because the fraction of cells expressing the foreign gene is very small, the mRNA expression level is also very low during transient expression after particle bombardment. In our studies with tobacco seedlings and leaves bombarded with DNA-coated particles, transiently expressed mRNA levels were too low to be detected by standard mRNA detection methods, i.e., Northern hybridization, primer extension and RNase protection assay.

Recently, a real time quantitative PCR system was developed (Heid et al., 1996; Gibson et al., 1996) that is based on continuous monitoring of PCR product accumulation through a fluorogenic probe, namely TaqMan probe (Holland et al.,

*Author for correspondence: e-mail: jo@bio.nagoya-u.ac.jp; fax: +81-52-789-3081; ph: +81-52-789-3087.

1991; Livak et al., 1995; Heid et al., 1996; Gibson et al., 1996). This system measures the initial concentration of template DNA by using the number of PCR cycles at which PCR amplification reaches a significant threshold level, rather than using the amount of final PCR products (Heid et al., 1996; Gibson et al., 1996).

In this study, a real time quantitative RT-PCR assay was applied to transgenic tobacco seedlings. The results demonstrate that this RT-PCR can be used to quantitate transient gene expression in tobacco cells into which the β-glucuronidase (GUS) gene had been introduced by particle bombardment.

Materials and Methods

Solutions

Phenol/chloroform: phenol:chloroform:isoamyl alcohol (25:24:1);
10x DNase buffer: 500 mM Tris-HCl (pH 7.5), 10 mM $MgCl_2$, 1 mg/mL BSA;
Antiformin: 1.5% sodium hypochlorite solution, 0.01% Triton X-100;
TE: 10 mM Tris-HCl (pH 8.0), 1 mM EDTA; Modified MS medium: standard MS medium containing 0.3% sucrose, 0.8% agar and 0.1% B5 vitamin stock (100 mg/mL myo-inositol, 10 mg/mL thiamin-HCl, 1 mg/mL nicotinic acid, 1 mg/mL pyridoxin-HCl); 10x TaqMan buffer: 500 mM KCl, 0.1 mM EDTA, 100 mM Tris-HCl (pH 8.3), and 600 nM ROX (6-carboxy-X-rhodamine).

Primers and a fluorogenic probe for RT-PCR

- GUS gene specific PCR primers:
  a sense strand primer is 5′-TACGGCAAAGTGTGGGTCAATAATCA-3′, and an antisense primer is 5′-CAGGTGTTCGGCGTGGTGTAGAG-3′.
- Fluorogenic probe:
  The TaqMan probe is 5′-CTTTAACTATGCCGGAATCCATCGCAGC-3′ with a reporter fluorescent dye [FAM (6-carboxyfluorescein)] at the 5′ end and a quencher dye [TAMRA (6-carboxy-tetramethyl-rhodamine)] at the 3′ end.

Plant materials

About 100 seeds, *Nicotiana tabacum* cv. Petite Havana SR1, are vortexed in 1 mL ethanol for 10 min. The ethanol is removed, 1 mL antiformin is added, and the seeds are vortexed for 10 min and washed 3 times in sterile water for 10 min each. The seeds are sown in a spot at the center of a modified MS agar plate, and incubated at 25°C under a regime of 16 h-L/8 h-D for about two weeks.

Particle bombardment

- Mix 0.5 μg pBI221 plasmid (CaMV35S::GUS) and 0.5 mg gold particles (1.5 to 3.0 μm diameter, Aldrich Chem.WI) well in 10 μl TE. Add 1.7 μl of 3 M sodium-acetate (pH 5.2) and 50 μl ethanol, then spin down to remove the supernatant. Rinse the pellet with 70% ethanol, then resuspend in 100 μl ethanol by brief sonication.

- Apply 4 µl aliquots of the above suspension to the particle gun (IDERA GIE-III, TANAKA Co., Ltd., Sapporo Japan), and bombard to the seedlings. One plate is bombarded 4 times.
- After bombardment, incubate the seedlings under continuous light at 25°C for the appropriate time period.
- Pour Liquid N_2 directly on the plate to freeze the seedlings.
- Grind the frozen tissues to a fine powder using a micro-dismembrator (B. Braun Biotech International, Germany). Ground tissue samples are store at –70°C.

GUS assay

An aliquot of the tissue powder is used for GUS assay with a chemiluminescence detection kit, GUS-Light (TROPIX, MA). The protein concentration is determined according to Bradford (1976) to normalize measured GUS activities.

RNA extraction

RNA is extracted according to the AGPC (acid guanidinium thiocyanate-phenol-chloroform) method (Chomczynski and Sacchi, 1987) with slight modifications. We routinely use ISOGENE (Nippon gene, Japan) instead of the guanidinium solution, as follows:

- Suspend the tissue powder (from ca. 0.1 g fresh weight) in 1 mL of ISOGEN (Nippon gene, Japan) and vortex for 30 sec.
- Put on ice for 5 min.
- Add 200 µl of chloroform and vortex for 15 min.
- Put on ice for 2 min.
- Centrifuge at 14,000 rpm for 15 min at 4°C.
- Transfer the upper layer to a fresh tube, and extract with an equal volume of phenol/chloroform once or twice.
- Add an equal volume of isopropanol, and centrifuge at 14,000 rpm for 15 min at 4°C.
- Discard the supernatant; add 100 µl of distilled water and vortex.
- Add 11 µl of 10 M LiCl and vortex, then store at –70°C for 1 h.
- Centrifuge at 14,000 rpm for 30 min at 4°C.
- Dissolve the pellet in 300 µl of distilled water.
- Add 30 µl of 3 M sodium acetate and 660 µl of ethanol, then store at –70°C for 10 min.
- Centrifuge at 14,000 rpm for 10 min at 4°C.
- Add 20 µl distilled water, and vortex to dissolve the pellet.
- To 15 µl of the above solution, add 3 µl of RNase-free DNase I (1U/µl) (PROMEGA Ltd.), 5 µl of DNase buffer and 27 µl of distilled water.
- Incubate at 37°C for 45 min.
- Add 150 µl of distilled water, then phenol/chloroform extraction.
- Add 200 µl of 4 M ammonium acetate and 800 µl of ethanol, then incubate at –70°C for 10 min.
- Centrifuge at 14,000 rpm for 10 min at 4°C, and rinse the pellet with 70% ethanol.

- Dissolve the pellet in 300 µl of distilled water, then ethanol precipitate again.
- Dissolve the pellet in 5 µl of distilled water.
- Determine the RNA concentration, and adjust it to 250 ng/µl.
- Check the integrity of the RNA by agarose gel electrophoresis.

RT-PCR

A real time quantitative RT-PCR analysis is carried out using ABI Prism 7700 Sequence Detection System.

- Mix 1 µl of RNA sample (250ng/mL), 1 µl of 10 mM antisense primer and 4.9 µl of distilled water in a 0.2 mL tube.
- Incubate at 70°C for 10 min and cool down to room temperature.
- Add 1.5 µl of 10x TaqMan Buffer, 3.6 µl of 25 µM magnesium chloride, 2 µl of 2.5 mM dNTP mixture and 1 µl of 50-fold diluted MuLV Reverse transcriptase (50U/µl).
- Incubate at 50°C for 30 min, then heat to 95°C for 5 min.
- Add 1 µl of 10x TaqMan Buffer, 2.4 µl of 25 mM magnesium chloride, 2 µl of 2.5 mM dNTP mixture, 0.5 µl of 10 µM sense and antisense primer, 0.5 µl of 5 µM TaqMan probe, 0.4 µl of AmpliTaq Gold DNA Polymerase (5.0U/µl) and 2.7 µl of distilled water. If fluorescent signal of ROX drifts during PCR cycles, add 2.5 µl of ROX stabilizer (PE Biosystems).
- Perform PCR: 95°C for 10 min, then 40 cycles of (95°C for 15 s and 57°C for 1 min).

Results and Discussion

A preliminary experiment was carried out to characterize real time quantitative RT-PCR in transgenic tobacco plants. Stable plant lines expressing GUS from the expression construct 35S::GUS were cultivated and total RNA extracted. A calibration curve was prepared using serial dilutions of the RNA template. The threshold PCR cycle, at which RT-PCR products from GUS mRNA accumulated to a critical level, was determined for samples in the range of 10 pg to 100 ng. The calibration curve was linear throughout this range (Figure 1), indicating that this method is a powerful and sensitive tool for RNA quantitation in plant systems. It should be especially useful for measuring extremely low abundance mRNA targets.

RT-PCR was also carried out in tobacco cells transiently expressing GUS after particle bombardment. Prior to RT-PCR, it was necessary to digest all DNA contamination in the RNA from bombarded cells using RNase-free DNase. In all cases, a control experiment is necessary to determine the fraction of the RT-PCR signal that comes from DNA contamination (i.e., assay in the absence of reverse transcriptase). It was also found that the success of the RT-PCR experiment depends on the choice of PCR primers and the amount of reverse transcriptase (excess enzyme can interfere with the RT-PCR signal). Thus, it is recommended that the amount of reverse transcriptase be carefully titrated and the optimal amount determined.

Quantitative RT-PCR was tested in tobacco cells transiently expressing GUS mRNA. The expression of GUS mRNA increased rapidly after particle

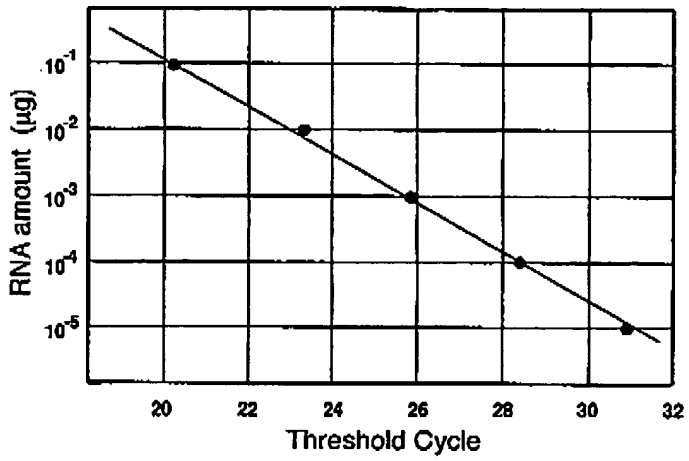

Figure 1. Calibration curve using RNA from stable tobacco cells expressing the GUS gene. Total RNA was prepared from transgenic tobacco plants carrying the 35S::GUS construct. RT-PCR was carried out with serial dilutions of total RNA (100 ng to 10 pg) and a GUS gene specific fluorogenic probe. Critical PCR cycle number (X-axis) is plotted versus initial RNA amount (Y-axis).

bombardment, reaching a maximum at 2 h and declining to 50% of the maximum by 5 h (Figure 2A). GUS enzyme activity was also measured (Figure 2B). In contrast, the enzyme activity increased to a maximum 8 h after gene transfer, and was maintained at a high level for up to 40 h.

To explain these kinetics, the half-life of GUS mRNA and protein should be considered. The half-life of GUS mRNA was reported to be less than 1 h in tobacco leaves (Weinmann et al., 1994) and no more than 3 h in tobacco protoplasts (Ohme-Takagi et al., 1993). The half-life of GUS protein was reported to be 3-4 d in green tobacco plants (Weinmann et al., 1994) and no more than 50 h in tobacco protoplasts (Jefferson et al., 1987). Thus, the most likely explanation for the kinetics of transient expression described in Figure 2 is the following: DNA is introduced by particle bombardment and immediately transported to the nucleus and transcribed. Subsequently, the foreign DNA is rapidly inactivated by modification or degradation, and the half-life of GUS mRNA and protein produced from the foreign gene is consistent with previous reports (i.e. 1-3 h for GUS mRNA and 2-4 d for GUS protein).

In summary, this study demonstrates the use of the real time quantitative RT-PCR to study transient gene expression in tobacco cells after particle bombardment. This is a powerful new approach for studies of gene expression in plant systems. It should be useful for studies of transcription, mRNA stability, protein translation and possible co-suppression or interference of foreign genes.

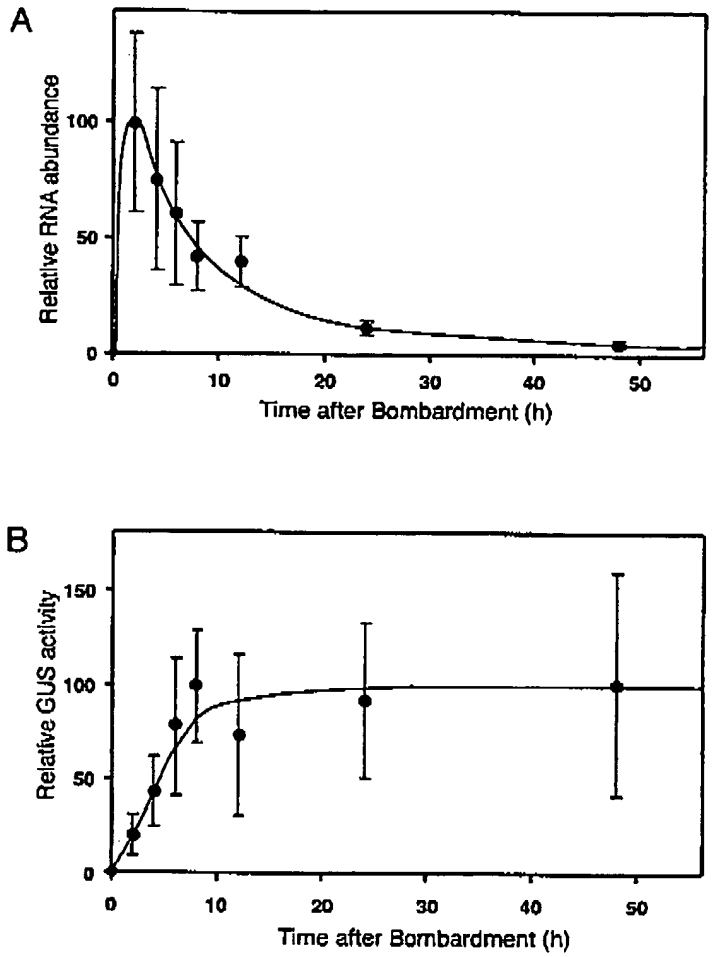

Figure 2. Kinetics of GUS gene transcription and GUS enzyme activity in tobacco cells transiently expressing the GUS gene. Samples were taken 2, 4, 6, 8, 12, 24 and 48 h after particle bombardment and protein and RNA samples isolated. The mean ± SD was calculated using data from 3 or 4 independent experiments. (A) GUS mRNA level was determined by quantitative RT-PCR, (B) GUS enzyme activity measured as described in the text.

Acknowledgements

We thank Dr. T. Kondo for use of an ABI PRISM 7700 Sequence Detection System, and Drs. M. Sugiura and M. Nakamura for useful discussions. This study

was supported in part by the Grants-in-Aid from the Ministry of Education, Science and Culture of Japan.

References

Bradford MM (1976) A rapid and sensitive method for the quantitation of microgram quantities of protein utilizing the principle of protein-dye binding. Anal Biochem 72: 248 254.

Chomczynski P and Sacchi N (1987) Single-step method of RNA isolation by acid guanidinium thiocyanate-phenol-chloroform extraction. Anal Biochem 162: 156-159.

Gibson UEM, Heid CA and Williams PM (1996) A novel method for real time quantitative RT-PCR. Genome Research 6: 995-1001.

Heid CA, Stevens J, Livak KJ and Williams PM (1996) Real time quantitative PCR. Genome Methods 6: 986-994.

Holland PM, Abramson RD, Watson R and Gelfand DH (1991) Detection of specific polymerase chain reaction product by utilising the 5'-3' exonuclease activity of Thermus aquaticus DNA polymerase. Proc Natl Acad Sci USA 88: 7276-7280.

Jefferson RA, Kavanagh TA and Bevan MW (1987) GUS fusions: β-glucuronidase as a sensitive and versatile gene fusion marker in higher plants. EMBO J 6: 3901-3907.

Livak KJ, Flood SJ, Marmaro J, Giusti W and Deetz K (1995) Oligonucleotides with fluorescent dyes at opposite ends provides a quenched probe system useful for detecting PCR product and nucleic acid hybridization. PCR Methods Applic 4: 357362

Ohme-Takagi M, Taylor CB, Newman TC and Green PJ (1993) The effect of sequences with high AU content on mRNA stability in tobacco. Proc Natl Acad Sci USA 90: 11811-5.

Weinmann P, Gossen M, Hillen W, Bujard H and Gatz C (1994) A chimeric transactivator allows tetracycline-responsive gene expression in whole plants. Plant J 5: 559-569.

Q&A Technically Speaking

By Abigail Farfan, M.A.
Promega Corporation

Eukaryotic Expression: Transfection and Reporter Vectors

Promega Corporation offers a variety of reagents for the stable and transient transfection of cells, and a number of reporter vectors designed for investigating the in vivo expression of promoter and enhancer sequences. Convenient assay systems have been developed for the analysis of reporter gene expression.

Q What are the TransFast™, Tfx™ and Transfectam® Reagents and how do they work?

TransFast™ Transfection Reagent[a] is comprised of the synthetic cationic lipid, N,N [bis (2-hydroxyethyl)-N-methyl-N-[2,3-di (tetradecanoyloxy)propyl] ammonium iodide and the neutral lipid L-dioleoyl phosphatidylethanolamine (DOPE). The TransFast™ Reagent is supplied as a dried lipid film that forms multilamellar vesicles upon hydration with water. The reagent neutralizes the negative charge of nucleic acids, allowing closer association of the liposome:DNA complex with the negatively charged cell membrane. Entry of the liposome:DNA complex into the cell may occur by the processes of endocytosis, or fusion with the plasma membrane via the lipid moieties of the liposome. Once inside the cell, the complexes often become trapped in endosomes and lysosomes. Endosomal disruption is facilitated by DOPE, which allows the complexes to escape into the cytoplasm. It is not known precisely how the liposome:DNA complex gains entry to the nucleus.

For a detailed description please refer to the *TransFast™ Transfection Reagent Technical Bulletin* #TB260.

The Tfx™ Reagents[b] are a mixture of a synthetic, cationic lipid molecule (N,N,N′,N′-tetramethyl-N,N′-bis(2-hydoxyethyl)-2,3-di (oleoyloxy)-1,4-butane-diammonium iodide) and the neutral lipid L-dioleoyl phosphatidylethanolamine (DOPE). The Tfx™-10, Tfx™-20 and Tfx™-50 Reagents all contain the same concentration of the cationic lipid component, but differ in the molar ratios of DOPE. The Tfx™ Transfection Reagents are suitable for stable and transient transfection of various cell lines, although each reagent exhibits differing transfection efficiencies depending on the cell type of interest.

The cationic lipid component of the Tfx™ Reagents consists of a positively charged head group attached to a lipid backbone by an ester linkage. The positively charged headgroups associate with the negatively charged nucleic acids, resulting in the formation of multilamellar vesicles. These vesicles presumably facilitate the transfer of nucleic acids into cells by interaction of the lipid backbone with the cell membrane.

For a detailed description please refer to the *Tfx™-10, Tfx™-20 and Tfx™-50 Reagents Technical Bulletin* #TB216.

Transfectam® Reagent[c] is composed of dioctadecylamidoglycyl spermine (DOGS), a synthetic cationic lipopolyamine molecule. The spermine group is covalently attached through a peptide bond to the lipid moiety. The strong positive charge contributed by the spermine headgroup gives the molecule a high affinity for DNA (10^5–$10^6 M^{-1}$), coating the DNA with a cationic lipid layer that facilitates binding to the cell membrane. This reagent is recommended for stable and transient transfections of a variety of cell types.

For a detailed description please refer to the *Transfectam® Reagent Technical Bulletin* #TB116.

Q How do I decide which transfection reagent to use for a particular cell type?

To help you decide which transfection reagent to use for the cell type of interest, please refer to the transfection assistant program available on the Promega web site at: www.promega.com/transfectionasst/. After the cell line of choice and the type of transfection to be performed (stable or transient) are entered, the program will display a list of transfection reagents and conditions that have been demonstrated to work with the cell type of interest. This information is based on experiments from various sources, including both published citations and data generated at Promega.

Q How do Promega's pGL3 Luciferase Reporter Vectors differ from the pGL2 Vectors?

The pGL3 Vectors[d,c] were created by improving the pGL2 Vectors[d]. The improvements included modifications to both the luciferase gene and the vector backbone.

Luciferase gene (*luc* to *luc+*) modifications:

1. Removal of a peroxisome targeting sequence.
2. Deletion of the consensus binding sequences for AP1, AP2, SP1, TGT-3 and LF-A1 genetic regulatory proteins.
3. Improvement of codon usage for mammalian and plant cells.
4. Removal of potential glycosylation sites.

For additional information please refer to reference 1 and to Table 1 in the *pSP-luc+ Vector Technical Bulletin* #TB208.

Table 1. Stability, Molecular Weights, Substrates and Sensitivities of Promega's Reporter Enzymes.

Reporter Enzyme	mRNA Half-Life	Protein Half-Life	Molecular Weight	Substrate	Sensitivity
Firefly Luciferase	6 hours (4)	3 hours (4,5) (mammalian)	61kDa monomer (6)	beetle luciferin (4,9)	1fg (10^{-20} moles)
Renilla Luciferase	unknown	5.3 hours at 40°C (5)	34/35kDa monomer (5,7,8)	coelentcrazine (5,8,11)	10fg (3×10^{-19} moles)
Beta-Galactosidase	unknown	20 hours	465kDa tetramer (9) (116kDa each)	ONPG (5,9)	10^4-10^5 molecules
CAT	6 hours (4)	50 hours (4)	80kDa tetramer (10) (20kDa each)	chloramphenicol (9)	510×10^7 molecules

Vector modifications:

1. The SV40 early poly(A) signal was replaced with the SV40 late poly(A) signal to increase the efficiency of transcription termination and polyadenylation of the luciferase transcripts.
2. A synthetic poly(A) and transcriptional pause site were placed upstream of the multiple cloning site to terminate spurious transcription, which may initiate within the vector backbone.
3. The small T intron was removed to prevent reduced reporter gene expression due to cryptic RNA splicing.
4. A Kozak consensus sequence was inserted to increase the efficiency of translation initiation of the luciferase gene.
5. A unique *Nco* I site, for the construction of N-terminal fusions with *luc+*, was added to the 5'-end of the *luc+* gene.
6. A unique *Xba* I site was created immediately downstream of the *luc+* gene for subcloning purposes.
7. The *Sma* I site was moved to an internal position in the multiple cloning site so that blunt-end inserts can be cleaved by restriction enzymes on either side.

For a detailed description please refer to the *pGL3 Luciferase Reporter Vectors Technical Manual* #TM033.

Q How does the relative activity of *Renilla* luciferase differ from that of firefly luciferase? What conditions are recommended for cotransfection of the two reporter vectors?

Firefly luciferase acts on beetle luciferin in the presence of ATP, magnesium and oxygen. *Renilla* luciferase, obtained from the sea

pansy *Renilla reniformis*, acts on coelenterazine in the presence of oxygen. Although their respective light outputs are similar, firefly luciferase has a molecular weight of 61kDa, and *Renilla* luciferase has a molecular weight of 36kDa. Therefore, when assaying equal mass amounts of the two enzymes, one is actually measuring 69% more molecules of *Renilla* luciferase. It has been empirically determined that, on a per mole basis, firefly luciferase provides approximately 53% greater luminescence intensity than *Renilla* luciferase when assayed using the Dual-Luciferase™ Reporter Assay(LR) chemistry. Please refer to reference 2 for additional information.

Trans effects between promoters on cotransfected plasmids can potentially affect reporter gene expression (3). This is of particular concern when either the control or the experimental reporter vector contain very strong promoter/enhancer elements. The TK, SV40 and CMV promoters in the pRL Vectors(h) are expressed at different levels in most mammalian cell types. The HSV-thymidine kinase promoter of pRL-TK is relatively weak and is most useful in providing neutral constitutive expression of the *Renilla* luciferase control reporter. The SV40 early and CMV immediate early promoter/enhancer regions provide high-level transcription and may be less suitable for coreporter applications involving experimental vectors with robust regulatory elements. In addition, the SV40 promoter and the CMV promoter contain transcription factor recognition sequences for SP1, AP1 and AP2. If the effects of such transcription factors on the experimental promoter are under investigation, the use of the SV40 and CMV control reporters is not recommended.

Transfection ratios of experimental vector to *Renilla* luciferase vector of 10:1, 50:1, 200:1 or greater are recommended to ensure independent genetic expression between the experimental and control reporter genes, to diminish or suppress the *trans* effects between promoter elements, and to control the level of expression of the cotransfected vectors.

For a detailed description please refer to the *Dual-Luciferase™ Reporter Assay System Technical Manual* #TM040.

Q What is the stability, molecular weight, substrate and sensitivity of each of Promega's Reporter Enzymes?

Stability, molecular weight, substrate and sensitivity data for Promega's firefly luciferase, *Renilla* luciferase, beta-galactosidase and chloramphenicol acetyltransferase (CAT) enzymes are listed in Table 1.

Q How do the pCAT®3 Reporter Vectors differ from the pCAT® Reporter Vectors?

Nine major modifications were made to the pCAT® Vectors to generate the pCAT®3 Vectors. These include:

1. The SV40 small T antigen intron was replaced with a chimeric intron 5′ of the CAT gene to enhance expression and decrease cryptic splicing.
2. The poly(A) signal for CAT was changed from the early to the late SV40 poly(A) signal for more efficient transcription termination and polyadenylation.
3. A synthetic poly(A) and transcriptional pause site was inserted 5′ of the CAT gene and multiple cloning sites to terminate spurious transcription upstream from the CAT gene.
4. A Kozak consensus sequence was created at the 5′-end of the CAT gene to optimize translation efficiency.
5. The multiple cloning sites were changed for compatibility with the pGL3 Vectors.
6. A f1 *ori* was included in the vector backbone for generation of single-stranded DNA.
7. A unique *Nco* I site was created in the Kozak sequence to facilitate subcloning.
8. A unique *Xba* I site was created just downstream of the CAT gene.
9. The *Eco*R I site was removed from within the CAT gene, resulting in the amino acid change Phe^{73} to Leu^{73}.

These modifications act to enhance CAT expression in transfected cells and increase cloning flexibility.

For a detailed description please refer to the *pCAT®3 Reporter Vectors Technical Manual* #TM036.

Q What is the Beta-Galactosidase Assay System?

The Beta-Galactosidase Assay System is a colorimetric assay system that detects beta-galactosidase enzyme activity in cells transfected with a vector expressing this enzyme (e.g., the pSV-Beta-Galactosidase Control Vector). The pSV-Beta-Galactosidase Control Vector is designed to be used as an internal control for transfection efficiencies when cotransfected into mammalian cells. Equal volumes of cell extract and Assay 2X Buffer, which contains the substrate ONPG (o-nitrophyl-beta-D-galactopyranoside), are mixed and incubated. The beta-galactosidase enzyme hydrolyzes the colorless substrate to o-nitrophenol, which is yellow. The reaction is inhibited with sodium carbonate, and the optical density is measured spectrophotometrically or with an ELISA plate reader at 420nm.

Q What reporter assays and protein assays are compatible with the Reporter Lysis Buffer (RLB), Passive Lysis Buffer (PLB) and Cell Culture Lysis Reagent (CCLR)?

A listing of reporter assays and protein assays that are compatible with each of Promega's lysis reagents and buffers is provided in Table 2. Note that the BSA standard curve generated for protein quantitation should always contain the same final volume as the sample. Volumes can be adjusted using the same lysis buffer as the sample.

Table 2. Reporter and Protein Assays Compatible with Cell Culture Lysis Reagent, Reporter Lysis Buffer and Passive Lysis Buffer.

Lysis Buffer	Compatible Reporter Assay	Protein Assay
Cell Culture Lysis Reagent (CCLR)	Luciferase only	First dilute the cell lysate 1:2 with water and use with BioRad #500-0116 DC protein assay or Pierce BCA protein assay #23225.
Reporter Lysis Buffer (RLB)	Luciferase Beta-Galactosidase CAT	Dilute the cell lysate 1:2 with water and use with BioRad DC protein assay #500-0116 (large-scale only) or Pierce BCA protein assay #23225. Alternatively, use 2-8µl of undiluted lysate with the Bradford assay.
Passive Lysis Buffer (PLB)	Luciferase Beta-Galactosidase CAT Dual-Luciferase™ Reagent	Pierce Coomassie® Plus protein assay (micro-scale). Use 100µl of the cell lysate with 1ml of the protein assay reagent.

REFERENCES

1. Sherf, B.A. and Wood, K.V. (1994) *Promega Notes* **49**, 14.
2. Sherf, B.A. *et al.* (1996) *Promega Notes* **57**, 2.
3. Farr, A. and Roman, A. (1991) *Nucl. Acids Res.* **20**, 920.
4. Thompson, J.F. *et al.* (1991) *Gene* **103**, 171.
5. Bronstein, I. *et al.* (1994) *Anal. Biochem.* **219**, 169.
6. *Luciferase Assay System Technical Bulletin* #TB101, Promega Corporation.
7. Matthews, J.C. *et al.* (1977) *Biochemistry* **16**, 85.
8. Lorenz, W.W. *et al.* (1993) In: *Bioluminescence and Chemiluminescence* John Wiley and Sons, 191.
9. Alam, J. and Cook, J.L. (1990) *Anal. Biochem.* **188**, 245.
10. Shaw, V.W. (1975) *Meth. Enzymol.* **43**, 737.
11. Lorenz, W.W. *et al.* (1991) *Proc. Natl. Acad. Sci. USA* **88**, 4438.

Ordering Information

Product	Size	Cat.#

TransFast™ Transfection Reagent	1.2mg	E2431
Tfx™ Reagents Transfection Trio	5.4mg	E2400
Tfx™-10 Reagent	9.3mg	E2381
Tfx™-20 Reagent	4.8mg	E2391
Tfx™-50 Reagent	2.1mg	E1811
Transfectam® Reagent	1mg	E1231
	0.5mg	E1232
pGL3-Control DNA	20µg	E1741
pGL3-Enhancer DNA	20µg	E1771
pGL3-Promoter DNA	20µg	E1761
pGL3-Basic DNA	20µg	E1751
pRL-TK Vector	20µg	E2241
pRL-CMV Vector[i]	20µg	E2261
pRL-null Vector	20µg	E2271
pRL-SV40 Vector	20µg	E2231
pCAT®3-Control Vector	20µg	E1851
pCAT®3-Enhancer Vector	20µg	E1881
pCAT®3-Promoter Vector	20µg	E1861
pCAT®3-Basic Vector	20µg	E1871
pSV-Beta-Galactosidase Control Vector	20µg	E1081
Luciferase Assay System[f]		E1500
Dual-Luciferase™ Reporter Assay System		E1910
CAT Enzyme Assay System with Reporter Lysis Buffer		E1000
Beta-Galactosidase Enzyme Assay with Reporter Lysis Buffer		E2000
Reporter Lysis Buffer, 5X	30ml	E3971
Passive Lysis Buffer, 5X	30ml	E1941
Luciferase Cell Culture Lysis Reagent	30ml	E1531

[a]The cationic lipid component of the TransFast™ Transfection Reagent is covered by U.S. Pat. No. 5,824,812 and pending foreign patents.

[b]The cationic lipid component of the Tfx™ Reagents is covered by U.S. Pat. Nos. 5,527,928, 5,744,625 and pending foreign patents.

[c]Transfectam is a registered trademark of BioSepra, Inc. The Transfectam® product was developed by J.P. Behr and J.P. Loeffler (under license from CNRS-ULP Strasbourg). Transfectam® Reagent is covered by U.S. Pat. No. 5,171,678.

[d]The method of recombinant expression of *Coleoptera* luciferase is covered by U.S. Pat. Nos. 5,583,024, 5,674,713 and 5,700,673.

[e]U.S. Pat. No. 5,670,356 has been issued to Promega Corporation for a modified luciferase technology.

[f]U.S. Pat. Nos. 5,283,179, 5,641,641, 5,650,289, and Australian Pat. No. 649289, have been issued to Promega Corporation for a firefly luciferase assay method, which affords greater light output with improved kinetics as compared to the conventional assay.

[g]U.S. Pat. No. 5,744,320 has been issued to Promega Corporation for quenching reagents and assays for enzyme-mediated luminescence.

[h]The cDNA encoding luciferase from *Renilla reniformis* is covered by U.S. Pat. No. 5,292,658 assigned to the University of Georgia Research Foundation, Inc., and sublicensed from SeaLite Sciences, Inc., Norcross, GA. The pRL family of *Renilla* luciferase cDNA vectors is for research use only. Commercial manufacture

would require a license from ScaLite Sciences, Inc.

(i)Covered under U.S. Pat. No. 5,168,062 assigned to the University of Iowa Research Foundation.

Protein Engineering vol.12 no.12 pp.1035–1040, 1999

COMMUNICATION

Attenuation of green fluorescent protein half-life in mammalian cells

Pete Corish and Chris Tyler-Smith[1]

CRC Chromosome Molecular Biology Group, Department of Biochemistry, University of Oxford, South Parks Road, Oxford OX1 3QU, UK

[1]To whom correspondence should be addressed. E-mail: chris@bioch.ox.ac.uk

The half-life of the green fluorescent protein (GFP) was determined biochemically in cultured mouse LA-9 cells. The wild-type protein was found to be stable with a half-life of ~26 h, but could be destabilized by the addition of putative proteolytic signal sequences derived from proteins with shorter half-lives. A C-terminal fusion of a PEST sequence from the mouse ornithine decarboxylase gene reduced the half-life to 9.8 h, resulting in a GFP variant suitable for the study of dynamic cellular processes. In an N-terminal fusion containing the mouse cyclin B1 destruction box, it was reduced to 5.8 h, with most degradation taking place at metaphase. The combination of both sequences produced a similar GFP half-life of 5.5 h. Thus, the stability of this marker protein can be controlled in predetermined ways by addition of the appropriate proteolytic signals.

Keywords: cyclin destruction box/green fluorescent protein/half-life/PEST sequence

Introduction

The green fluorescent protein (GFP) from the jellyfish *Aequoria victoria* provides a visual marker that can be used in a wide variety of organisms (Chalfie *et al.*, 1994; Tsien, 1998). The wild-type protein has been significantly improved for use in mammalian cells by the incorporation of mutations such as S65T and F64L, which change the absorption spectrum and increase the rate of fluorophore formation (Heim *et al.*, 1995) and by 'humanizing' the codon usage (Zolotukhin *et al.*, 1996). GFP folds into a unique, compact structure, the β-can (Ormö *et al.*, 1996; Yang *et al.*, 1996), that is strongly resistant to chemical denaturation (Ward and Bokman, 1982) and is observed to be stable in most cells (Cubitt *et al.*, 1995). This is well suited to purposes such as marking cell lineages, but for monitoring dynamic processes such as gene expression or chromosome transmission, a less stable protein with a more rapid turnover would be more suitable.

The role of controlled protein degradation as a method of regulating many cellular biochemical processes has only recently been fully appreciated and the pathways involved in the accurate targetting of proteins for proteolysis are an increasingly important area of study. Failure of the key components in these pathways can be causative in human disease (Kishino *et al.*, 1997; Matsuura *et al.*, 1997) and responsible for incomplete cell-cycle progression (Ghislain *et al.*, 1993; Finley *et al.*, 1994; Pu and Osmani, 1995). Central to this process of degradation is the 26S proteosome, a 2000 kDa multi-protein complex which is distinct from the compartmentalized lysosomal proteolysis machinery and is responsible for the ATP-dependent turnover of 80–90% of the cell's protein content (Lee and Goldberg, 1998). Proteins are generally, but not exclusively, identified for systematic degradation in the proteosome by ubiquitination. The specificity of this process is in part defined by the action of a family of E2-ubiquitin conjugating enzymes, which catalyse the final ubiquitin addition, but is also conferred by sequence motifs in the target protein which act as proteolytic signals.

One such motif, the PEST sequence, is found extensively in short-lived proteins including metabolic enzymes, transcription factors and their regulators, signalling pathway components and certain cyclins (Rechsteiner and Rogers, 1996). PEST sequences are enriched for proline, glutamate, serine and threonine in a negatively or neutrally charged background and removal of this region from short-lived proteins results in more stable derivatives (Tyers *et al.*, 1992; Pu and Osmani, 1995; Tsurumi *et al.*, 1995). The metabolic enzyme ornithine decarboxylase (ODC) is a key regulatory control point in polyamine biosynthesis and is regulated by 26S proteosome degradation, albeit without prior ubiquitination, which is mediated by two PEST regions. Transfer of the carboxy-terminal ODC PEST region to a reporter enzyme, dihydrofolate reductase, resulted in an increased turnover rate of the DHFR protein (Loetscher *et al.*, 1991).

An alternative mechanism of targetting proteins for rapid degradation is the 'cyclin destruction box' (CDB), which leads to ubiquitination and degradation of A- and B-type cyclins by the 26S proteosome at the end of mitosis. This process is promoted by the anaphase promoting complex (APC), which possesses E3-ubiquitin ligase activity, as part of its role as regulator of the metaphase–anaphase transition checkpoint. Transfer of the CDB to protein A led to destabilization of this protein in *Xenopus* extracts (Glotzer *et al.*, 1991).

We wish to use destabilized GFPs to assay chromosome transmission in mammalian cells. We therefore engineered fusion proteins that link GFP to an ODC PEST sequence and a cyclin B1 destruction box region, to determine if these signals can reduce the resistance of wild-type GFP to proteolysis. The stabilities of these fusion proteins in mouse cells were compared with that of unmodified GFP.

Materials and methods

Plasmid construction

All constructs were produced in a modified version of the high-level mammalian constitutive expression vector pCAGG-Zeo (Niwa *et al.* 1991), allowing coordinated expression of GFP and Zeocin (Invitrogen) drug resistance from a single transcript incorporating an internal ribosome entry site. The 'humanized' S65T variant of GFP (Heim *et al.* 1995) was cloned as a 720 bp *Ecl*136II/*Xba*I fragment into *Eco*RI-cut pCAGG-Zeo, after end-filling of recessed 3′ ends. In the resulting plasmid, the GFP gene was flanked by reconstituted *Eco*RI sites, the downstream 3′ site was inactivated to facilitate

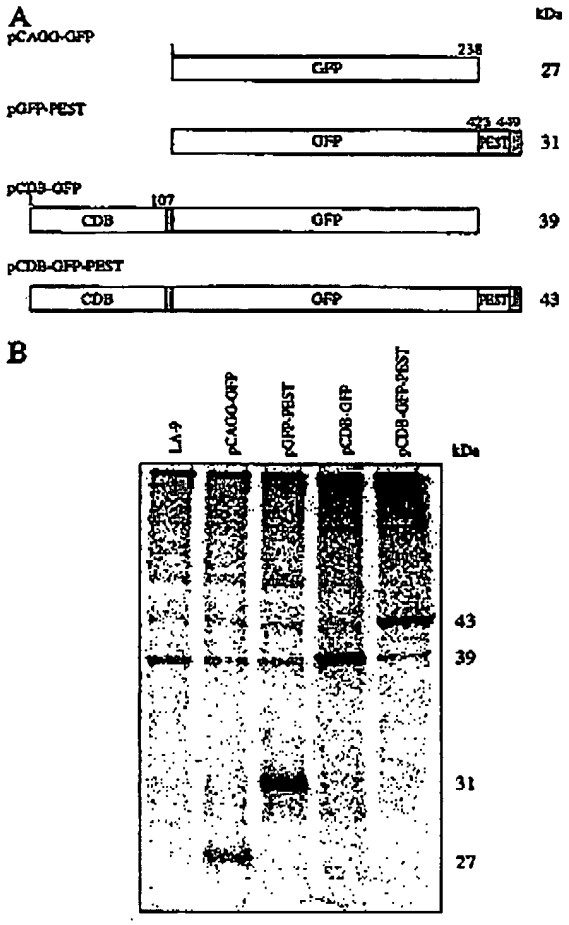

Fig. 1. (A) Structures of the variant GFP constructs expressed from the pCAGG-Zeo vector and their predicted protein product sizes. Additional amino acid sequences, resulting from cloning procedures, not found in either GFP, murine ODC PEST or cyclin destruction box (CDB), are shown shaded. Amino acid numbering refers to residue positions in the original mouse ODC and cyclin B1 proteins and not to the GFP fusions. (B) SDS–PAGE analysis of immunoprecipitated ^{35}S-radiolabelled GFP variants from stably transformed LA-9 cell lines.

subsequent cloning steps. The plasmid was further modified by removal of a 760 bp region containing a polyoma virus origin of replication resulting in the 7.8 kb plasmid pCAGG–GFP.

The carboxy-terminal PEST sequence corresponding to codons 423–449 of the mouse ornithine decarboxylase gene (mODC) was amplified by PCR from LA-9 genomic DNA using the primers ODC-1 (5′-GAG CTG TAC AAG CAT GGC TTC CCG CCG GAG-3′) and ODC-2 (5′-GAG CTG TAC ATT AAC GGT CCA TCC CGC TCT C-3′) which contain *Bsr*GI sites (underlined). A 100 bp product was isolated and cloned into the unique *Bsr*GI site at the 3′ end of the GFP gene in pCAGG–GFP to produce an in-frame fusion of the PEST sequence to the carboxy terminal of the GFP protein. Sequence analysis of this plasmid, pGFP–PEST revealed a single base deletion in the PCR-derived fragment at the intended TAA termination codon (in bold). This frameshift mutation resulted in the addition of a sequence of nine amino acids (NVQVKLPRL), not found in either mODC or GFP, before a TAG termination codon was reached (Figure 1A).

Cell-cycle specific degradation of GFP was achieved using an amino-terminal fusion of the mouse cyclin B1 destruction box (CDB) motif to GFP. A 348 bp fragment from the 5′ end of mouse cyclin B1 was amplified by PCR from embryonic stem cell genomic DNA using primers CYC-1 (5′-CGG AAT TCT CTG ATT TTG GAG GAG CCA TG-3′) and CYC-2 (5′-ATG AAG CTT TTC AAG TTC AGG TTC AGG C-3′) which included *Eco*RI and *Hin*dIII restriction sites (underlined), respectively. The resulting amplified product was cloned, after digestion, into partial *Hin*dIII/*Eco*RI-cut pCAGG–GFP producing an in-frame fusion to the N-terminal end of GFP, resulting in plasmid pCDB–GFP. Five amino acids (KLAAT), derived from vector sequences, separate the 3′ end of the cyclin fragment from the original GFP initiation codon. Sequencing confirmed the cyclin sequence was free of PCR-induced mutations and corresponded to a published variant murine B1 cyclin (Hanley-Hyde *et al.*, 1992).

Sub-cloning of the mODC PEST sequence from pGFP–PEST into the *BsrGI* site of pCDB–GFP resulted in plasmid pCDB–GFP–PEST in which both putative proteolytic targetting signals were incorporated in the same GFP fusion protein.

Cell culture and transfections

Mouse cell line LA-9 was maintained in DMEM supplemented with 10% fetal calf serum (Globepharm) and selection for drug-resistant lines made with 600 μg/ml Zeocin. Cell lines with stable integrations of the various GFP constructs were produced by electroporation of LA-9 cells with 10 μg of linearized plasmid DNA. Colonies were visualized and selected for GFP expression using an inverted fluorescence microscope (Leica DMIRB) with an FITC filter set (Leica I3) and several independent colonies chosen for expansion and subsequent analysis. For analysis of the CDB–GFP dynamics, cells were synchronized in S phase by treatment with 2 μg/ml aphidicolin (Sigma) for 16 h. FACS analysis of GFP fluorescence was performed on a Becton-Dickinson Facscalibur machine using the supplied FITC filter set.

Metabolic labelling of proteins and immunoprecipitation

GFP half-life was determined by immunoprecipitation of pulse-labelled proteins. Approximately 1×10^6 cells (30–40% confluent in 10 cm plates) were incubated with 50 μCi of ^{35}S-labelled methionine (TranSLabel, ICN Pharmaceuticals) in 4 ml of methionine-deficient DMEM (Sigma) for 4 h at 37°C to pulse label all proteins including GFP. After this time, the medium was replaced with fully supplemented, unlabelled DMEM and an initial sample taken to determine the incorporation of the ^{35}S-labelled methionine at the start of the experiment. Between five and seven further samples were taken during the next 48 h chase period at approximately 6 h time points.

For each time point, cells were lysed in 1 ml of TETN250 buffer (25 mM Tris–Cl pH 7.5, 5 mM EDTA, 1% Triton X-100, 250 mM NaCl, 1 mM PMSF), the soluble fraction pre-cleared with rabbit serum and GFP selectively immunoprecipitated using 1 μl of undiluted rabbit anti-GFP polyclonal antibody (IgG fraction; Clontech). GFP–antibody complexes were collected using a 10% formalin-fixed *Staphylococcus aureus* cell suspension (Immunoprecipitin; Life Technologies) and washed with lysis buffer before separation on 12% SDS–PAGE gels by standard methods (Harlow and Lane, 1988). Gels were dried under vacuum after fixing in methanol–acetic acid–glycerol and electronic autoradiography was carried out using an Instant Imager (Packard Bell Instruments). The total radioactivity in bands corresponding to GFP or its tagged

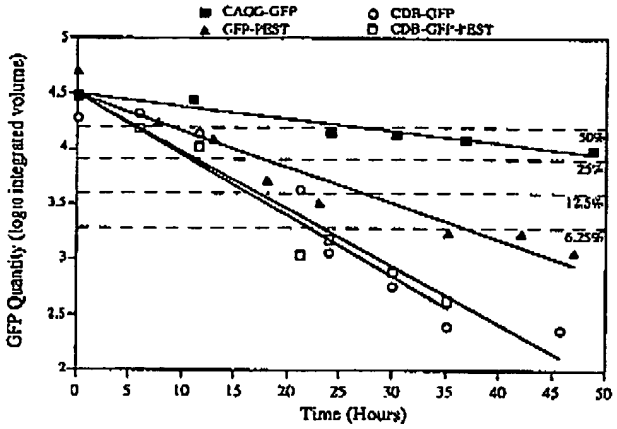

Fig. 2. GFP stability is reduced in variants carrying proteolytic signal sequences. Linear regression lines for each of the four tested GFP variants are shown (r^2 = 0.937, 0.93, 0.919 and 0.964, respectively). Horizontal dashed lines indicate 50% decreases in activity on a log scale, representing one to four half-lives. No 48 h time point is displayed for CDB–GFP–PEST as band activity levels were indistinguishable from background.

variants was calculated by volume integration using the built-in software after background correction. The GFP half-life was calculated by linear regression analysis of log(total radioactivity per band) against time.

Results

Stably transformed cell lines containing each of the three fusion protein constructs or the S65T unmodified CAGG–GFP (Figure 1A) were produced in mouse LA-9 cells. The integrity of the fusion proteins produced was determined both by fluorescence microscopy and by immunoprecipitation. Visually, all cell lines displayed green fluorescence, which indicated that they were expressing the GFP fusions although with intensity levels and distribution patterns specific for each construct (described below). Immunoprecipitation of ^{35}S-labelled proteins using a polyclonal anti-GFP antibody produced bands at the predicted size for each of the fusion proteins, from GFP at 27 kDa (Tsien, 1998) to the combination-tagged CDB–GFP–PEST variant at 43 kDa (Figure 1B). Several additional bands, 39 kDa or larger, were also observed even in the parental untransfected LA-9 control lane and represent non-GFP proteins with affinity for the polyclonal antibody. While one of these bands co-migrates with the CDB–GFP fusion protein, the relative intensity of the bands indicates that this was an unrelated band and did not result from contamination of the parental cell line, which was consistently non-fluorescent.

Immunoprecipitated samples of pulse-chase labelled protein extracts were taken over a 48 h period to determine the stabilities of each of the fusion proteins (Figure 2). As predicted from the structure, CAGG–GFP was a stable protein whose destruction followed first-order kinetics with a half-life of approximately 26 h. The fusion protein containing the C-terminal mouse ODC PEST sequence was also degraded with first-order kinetics, but at an increased rate, resulting in a reduced half-life of 9.8 h. This represents a significant destabilization of the protein of 2.6-fold compared to CAGG–GFP.

There was no significant difference in fluorescence intensities between GFP and GFP–PEST lines when examined visually despite the increased turnover of the fusion protein. This observation was quantitatively confirmed by subsequent FACS analysis and indicates that the steady-state levels of the protein are the same. This was not the case for CDB fusion proteins that showed highly variable levels of expression between individual cells from unsynchronized cultures of the same clonal line. In particular, cells undergoing mitosis (as determined by a 'rounding off' phenotype) or cells which had recently completed cytokinesis appeared non-fluorescent and revealed a bimodal distribution in FACS analysis (Figure 3D). The left-hand peak in this profile corresponded to cells undergoing mitosis which, nevertheless, showed minimal levels of fluorescence 2–3 times brighter than the non-fluorescent parental LA-9 cells (Figure 3B). During this period of the cell cycle, many proteins are being degraded by the 26S proteosome and so complete removal of the excessive amounts of GFP produced may be hindered by saturation of the degradation machinery.

The cyclin destruction box produced the most significant effect on protein stability, as the CDB–GFP fusion protein had a half-life of 5.8 h averaged over the 48 h sample period (Figure 2). However, this rate was not constant during this time, as demonstrated when synchronized, rather than unsynchronized, cultures were examined (Figure 3A). In this case, the majority of GFP turnover was seen to occur as cells entered mitosis, during which the GFP half-life was 4.9 h. Outside the mitotic phase, the protein remained predominantly stable. Thus, the figure of 5.8 h reflects the fact that not all cells in the unsynchronized culture are actively degrading GFP to the same extent.

The addition of the PEST motif to this CDB–GFP protein marginally reduced the average half-life further to 5.5 h. The outstanding feature of this latter 'combination' fusion is that overall levels of fluorescence were the lowest for any of the fusions, such that no labelled protein could be detected on the final time point sample. Also, FACS analysis of unsynchronized cells expressing CDB–GFP–PEST showed a bimodal distribution of fluorescence where the lower peak coincided with the non-fluorescent negative control (data not shown). Thus, addition of the PEST region does not appear to make a significant difference to fluorescence when protein levels are non-limiting; at lower concentrations, its effect is more evident.

The most prominent consequence of fusing the GFP sequence to the cyclin destruction box was highlighted through a time-dependent analysis of fluorescence development and decay in cells from synchronized culture (Figure 3A and F). Cells from lines containing either the CAGG–GFP or CDB–GFP variants were blocked in S phase using the DNA synthesis inhibitor aphidicolin (Sourlingas and Sekeri-Pataryas, 1996). The FACS profiles of these cells immediately after removal of the synthesis block showed similar distributions of fluorescence intensities, with wild-type GFP being slightly higher (Figure 3C and E). However, over a period of 26 h, corresponding to approximately one and a half cell cycles for LA-9 cells, the population profiles differed dramatically. In order to measure the early stages of fluorescence loss, observed as an initial moderate shift in the FACS profile peak to the left in Figure 3D, cells were defined as fluorescent if they exhibited a relative fluorescence intensity of ≥200 units. Inevitably, below this threshold some cells were included as non-fluorescent despite expressing significant levels of GFP. By this criterion, the percentage of fluorescent cells remained constant (80–85%) in the line expressing CAGG–GFP, whereas the CDB–GFP line

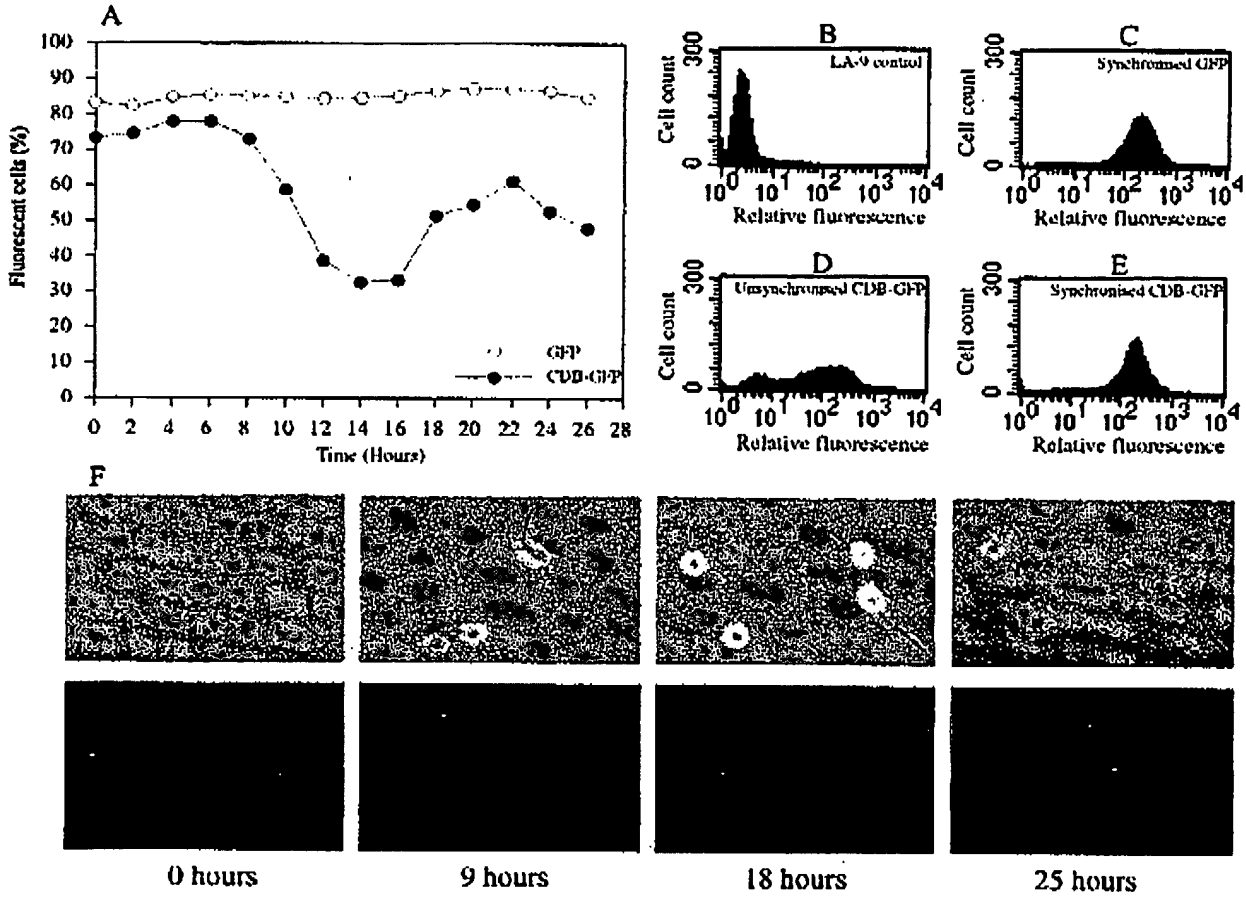

Fig. 3. (A) Cyclical changes in fluorescence intensity in aphidicolin S-phase-synchronized cultures of LA-9 cells expressing the CDB–GFP fusion protein compared with wild-type GFP. Fluorescence was measured as the portion of cells 200× brighter or greater than the non-fluorescent LA-9 parental line. This results in a percentage of cells (15–20%) from the left-most tail of the positive control being classed as non-fluorescent. (B) FACS profile of unsynchronized untransfected LA-9 cells used as the negative control (mean fluorescence = 2.9). (C) FACS profile of S-phase-synchronized cells expressing CAGG–GFP (mean fluorescence = 227). (D) and (E) FACS profiles of unsynchronized and S-phase-synchronized cells expressing CDB–GFP (mean fluorescence = 124, with geometric mean of 53.7 and 170, respectively). (F) Phase contrast (upper panels) and fluorescent (lower panels) images of a pair of cells, expressing the CDB–GFP fusion protein, photographed over a 25 h period, illustrating the dynamics of GFP fluorescence throughout the cell cycle.

showed a loss of fluorescence down to 30% as the synchronized cells entered mitosis. Fluorescence levels increased subsequently as cells progressed through G1 and S phase before a second decrease occurred as cells entered their second mitotic division. The reduced peak in fluorescence levels during this second cycle (62% compared with 78%) results from the loss of synchronization in the population after this length of time. These dynamic changes in CDB–GFP fluorescence with cell cycle progression are illustrated in Figure 3F, in which each cell of a synchronized pair undergoes mitosis resulting in reductions in fluorescence levels. At the four-cell stage, once the cells are in interphase, fluorescence levels have returned to a maximum and are comparable between all cells. Although it is not possible from these data to establish the exact timing of these changes with respect to the cell cycle, the pattern is consistent with that reported for normal cyclin B1 accumulation and degradation (Glotzer *et al.*, 1991).

Discussion

The most notable impact of green fluorescent protein technology to date in cell biology has been its use in fusion proteins for monitoring a specific protein's localization, trafficking and processing (Corbett *et al.*, 1995; Rizzuto *et al.*, 1996; Oatey *et al.*, 1997; Tsien, 1998). For these purposes, GFP already has been engineered to be brighter and to exhibit a wider range of excitation and extinction frequencies, which are amenable to double labelling studies (Tsien, 1998). However, further development of GFP will undoubtedly take the direction of utilizing GFP *per se* as an indicator of cellular state, as opposed merely to conferring fluorescence on previously non-fluorescent proteins of interest. It is to this class of modification that the GFP variants described in this work belong.

The reduction in GFP stability seen in the mODC PEST-tagged variant, while significant, still places GFP at the higher end of stability compared with more traditional reporters of gene activity such as luciferase which has a half-life of approximately 3 h (Thompson *et al.*, 1991). In addition, the lack of enzymatic amplification of a signal with GFP means that its sensitivity is limited, as cytoplasmic concentrations of approximately 1 μM are required to distinguish signal from auto-fluorescent background (Niswender *et al.*, 1995). However, as most enzymatic methods involve cell disruption, this

improvement in using GFP non-invasively with a shorter half-life will be suitable for many applications. In particular, for monitoring chromosome transmission, where expression of GFP to readily detectable levels is not problematic, the shorter half-life means that parentally derived cytoplasmic GFP is removed quickly, allowing the measurement of *de novo* GFP synthesis from the daughter cells.

GFP may yet be a viable alternative for *in vivo* gene expression studies if the destabilization can be improved to reduce the half-life further. A destabilized GFP variant, d2GFP, has recently been described (Li *et al.*, 1998) which utilizes a PEST region very similar to that used in this work. However, the reported half-life of this variant is 2 h and further reports of a 1 h variant (d1GFP) are based on fluorescence measurements, not biochemical purification. The discrepancy between those claims and the results presented here has been investigated to distinguish between cell differences, experimental protocols and intrinsic properties of the GFP variants used. We have confirmed the increased rate of degradation of the d1GFP variant, compared with the GFP–PEST described here (data not shown), and using the more accurate method of pulse-chase labelling we have determined its half-life to be 50 min in human HT1080 cells.

This result is remarkable considering the overall homology between the two mODC PEST sequences used. The d2GFP variant is extended compared with GFP–PEST by only 13 amino acids, but the core PEST region is maintained between both. This clearly implicates 'non-PEST motif' residues as having a major contributory role to the rapid turnover of the mouse ornithine decarboxlase protein ordinarily. What is more significant, however, is that in the most unstable d1GFP variant the conserved Glu residues in the PEST region are mutated to Ala. While these changes would theoretically predict a weaker PEST motif, in practice the alterations result in a 50% reduction in protein stability. Consequently, the presence of a PEST motif within a protein merely implies a propensity to instability and cannot indicate the magnitude of the degradation rate even when close to or identical with the consensus PEST sequence.

While the patterns of protein degradation for the cyclin–GFP fusion proteins are more complex than the simple linear profiles obtained with the PEST fusions, these variants are potentially useful as non-invasive indicators of cell-cycle status. The FACS profile of unsynchronized cells expressing these proteins (Figure 3D) is an indirect measurement of the proportion of cells in defined stages of the cell cycle. Although more detailed investigation of the correlation between fluorescence levels and cellular status is necessary, the lower peak of the fluorescence distribution corresponded broadly to mitotic and early G1 cells. Therefore, this form of GFP could be used as an alternative to procedures, such as propidium iodide staining, which require fixation with concomitant cell death. Indeed, in the cell synchronization experiments described (Figure 3A–E), the fluorescence levels were a direct indication of the efficiency of the aphidicolin treatment.

However, it is still debatable as to how accurately GFP fluorescence intensity is a reliable indicator of GFP levels in a cell. Two factors that significantly affect the fluorescent properties of GFP, namely the requirement for post-translational oxidative fluorophore formation and the sensitivity to cellular pH, could result in fluorescence intensities being lower than actual GFP concentration. Western analysis indicates that a good correlation exists between fluorescence intensity and protein concentration (Li *et al.*, 1998), but does not distinguish between immature, non-fluorescent and mature, fluorescent forms of GFP.

Considering this correlation between fluorescence levels and protein content, it is paradoxical that cell lines containing the unstable GFP–PEST construct (half-life 9.8 h) have fluorescence intensities not significantly different to those of lines containing its more stable GFP counterpart (half-life 26 h). Differences in steady-state protein levels between these lines would predict that the more unstable lines are also the least intense for GFP fluorescence, contrary to the actual observation. A similar observation was reported for the d2GFP variant (Li *et al.*, 1998), although in our experimental system lines containing this construct evidently displayed weaker fluorescence both in FACS analysis and by microscopy. Although this could indicate that non-fluorescent immature GFP molecules are preferentially degraded, we believe this to be unlikely. Instead, it is probable that proteolytic products from 26S proteosome activity maintain a degree of fluorescence (Tsien, 1998) but are not detected by the immunoblot technique used to measure half-life, thereby increasing the apparent GFP concentration. Thus, reduction in fluorescence intensity is proportional to a decrease in GFP half-life, but not to the same magnitude. The d1GFP variant that is 30 times more unstable than the wild-type GFP is, nonetheless, only ~70–80% less intense by FACS analysis.

The results also shed some light on the biology of proteolytic signalling itself. The GFP–PEST fusion construct has been tested in human HT1080 and HeLa-S3 cell lines where the fusion protein localized to give a punctate pattern. The distribution of GFP foci appeared limited to the cytoplasm, partially concentrated around the nuclear envelope (data not shown). This phenotype was only seen in LA-9 cells when the brighter EGFP variant was fused to mouse ODC PEST, although the phenotype was less pronounced than in human cells. This mottled pattern is unlikely to be due to sub-cellular localization of the 26S proteosome, which is known to be found in both the nucleus and cytoplasm (Coux *et al.*, 1996), but may represent natural sequestering of proteins marked for degradation away from the active cellular protein conterparts. Equally, the phenotype may be artefactual, with the very high levels of expression from the pCAGG vector resulting in protein aggregation complexes.

The distribution of the CDB–GFP protein was also consistent with known cyclin B1 characteristics (Hagting *et al.*, 1998). A pronounced nuclear localization was observed in mouse and human HT1080 cells (Figure 3F, 0 h, lower panel). Nuclear-cytoplasmic translocation is a normal feature of cyclin B1 expression and is mediated by a putative cytoplasmic retention or nuclear export signal between residues 129 and 157 (Hagting *et al.*, 1998; Toyoshima *et al.*, 1998) which is absent from the CDB–GFP construct (Figure 1A). In this respect, CDB–GFP is a useful starting point for the *in vivo* analysis of the 5′ region of the gene which is responsible for the dynamic movement of the cyclin B1 protein throughout the cell cycle.

In conclusion, it is evident from the results using the PEST and CDB fusions that the barrel-like structure of GFP is not refractory to major modifications that alter the basic properties of GFP biology. In these examples, GFP stability can be permanently compromised by the addition of the appropriate proteolytic signal sequences. Engineering opportunities are, however, limited to the carboxy- and amino-terminal ends for GFP, as internal modifications destroy the protective barrel structure and expose the fluorophore rendering it non-fluores-

cent (Dopf and Horiagon, 1996). However, the ease by which new derivatives can be produced and tested directly in living cells will allow GFP to be tailored to a variety of individual uses.

Acknowledgements

We thank Elizabeth Burns for plasmid donations and Steve Kain and Jason Li of Clontech for sharing unpublished results. P.C. was supported by the MRC and C.T.-S. by the Cancer Research Campaign.

References

Chalfie,M., Tu,Y., Euskirchen,G., Ward,W.W. and Prasher,D.C. (1994) *Science*, 263, 802–805.
Corbett,A.H., Koepp,D.M., Schlenstedt,G., Lee,M.S., Hopper,A.K. and Silver,P. (1995) *J. Cell Biol.*, 130, 1017–1026.
Coux,O., Tanaka,K. and Goldberg,A.L. (1996) *Annu. Rev. Biochem.*, 65, 801–847.
Cubitt,A.B., Heim,R., Adams,S.R., Boyd,A.E., Gross,L.A. and Tsien,R.Y. (1995) *Trends Biochem. Sci.*, 20, 448–455.
Dopf,J. and Horiagon,T.M. (1996) *Gene*, 173, 39–44.
Finley,D., Sadis,S., Monia,B.P., Boucher,P., Ecker,D.J., Crooke,S.T. and Chau,V. (1994) *Mol. Cell Biol.*, 14, 5501–5509.
Ghislain,M., Udvardy,A. and Mann,C. (1993) *Nature*, 366, 358–362.
Glotzer,M., Murray,A.W. and Kirschner,M.W.(1991) *Nature*, 349, 132–138.
Hagting,A., Karlsson,C., Clute,P., Jackman,M. and Pines,J. (1998) *EMBO J.*, 17, 4127–4138.
Hanley-Hyde,J., Mushinski,J.F., Sadofsky,M., Huppi,K., Krall,M., Kozak,C.A. and Mock,B. (1992) *Genomics*, 13, 1018–1030.
Harlow,E. and Lane D (1988) *Antibodies: a Laboratory Manual*. CSHL, New York.
Heim,R., Cubitt,A.B. and Tsien,R.Y. (1995) *Nature*, 373, 663–664.
Kishino,T., Lallande,M. and Wagstaff,J. (1997) *Nature Genet.*, 15, 70–73.
Lee,D.H. and Goldberg,A.L. (1998) *Trends Cell Biol.*, 8, 397–403.
Li,X., Zhao,X., Fang,Y., Jiang,X., Duong,T., Fan,C., Huang,C.-C and Kain,S.R. (1998) *J. Biol. Chem.*, 273, 34970–34975.
Loetscher,P., Pratt,G. and Rechsteiner,M. (1991) *J. Biol. Chem.*, 266, 11213–11220.
Matsuura,T., Sutcliffe,J.S., Fang,P., Galjaard,R.-J., Jiang,Y.-H., Benton,C.S., Rommens,J.M. and Beaudet A.L. (1997) *Nature Genet.*, 15, 74–75.
Niswender,K.D., Blackman,S.M., Rohde,L., Magnuson,M.A. and Piston,D.W. (1995) *J. Microsc.*, 180, 109–116.
Niwa,H., Yamamura,K. and Miyazaki,J. (1991) *Gene*, 108, 193–200.
Oatey,P.B., VanWeering,D.H.J., Dobson,S.P., Gould,G.W. and Tavare,J.M. (1997) *Biochem. J.*, 327, 637–642.
Ormö, M., Cubitt,A.B., Kallio,K., Gross,L.A., Tsien,R.Y. and Remington,S.J. (1996) *Science*, 273, 1392–1395.
Pu,R.T. and Osmani,S.A. (1995) *EMBO J.*, 14, 995-1003 .
Rizzuto,R., Brini,M., DeGiorgi,F., Rossi,R. and Heim,R., Tsien,R.Y. and Pozzan,T. (1996) *Curr. Biol.*, 6, 183–188.
Sourlingas,T.G. and Sekeri-Pataryas,K.E. (1996) *Anal. Biochem.*, 234, 104–107.
Thompson,J.F., Hayes,L.S. and Lloyd,D.B. (1991) *Gene*, 103, 171–177.
Toyoshima,F., Moriguchi,T., Wada,A., Fukuda,M. and Nishida,E. (1998) *EMBO J.*, 17, 2728–2735.
Tsien,R. (1998) *Annu. Rev. Biochem.*, 67, 509–544.
Tsurumi,C. *et al.* (1995) *Mol. Cell Biol.*, 15, 5682–5687.
Tyers,M. Tokiwa,G., Nash,R. and Futcher, B. (1992) *EMBO J.*, 11, 1773–1784.
Ward,W.W. and Bokman,S.H. (1982) *Biochemistry*, 21, 4535–4540.
Yang,F., Moss,L.G. and Phillips,G.N.,Jr. (1996) *Nature Biotechnol.*, 14, 1246–1251.
Zolotukhin,S., Potter,M., Hauswirth,W.W., Guy,J. and Muzyczka,N. (1996) *J. Virol.*, 70, 4646–4654.

Received December 11, 1998; revised August 26, 1999; accepted September 1, 1999